EUROPEAN COMMISSION

Community Research

SEVENTH FRAMEWORK PROGRAMME

ARCHER

Collaborative Project (CP)

Co-funded by the European Commission under the Euratom Research and Training Programme on Nuclear Energy within the Seventh Framework Programme

Grant Agreement Number : 269892

Start date : 01/02/2011 Duration : 48 Months

www.archer-project.eu

Archer

Advanced Reactor for Cogeneration of Heat & Electricity-R&D

Predictive Assessment of dust production and fission product release for HTR-10

Authors : André Xhonneux (FZJ), Stephan Struth (FZJ), Claudia Druska (FZJ)

ARCHER - Contract Number: 269892
Advanced High-Temperature Reactors for Cogeneration of Heat and Electricity R&D
EC Scientific Officer: Dr. Panagiotis Manolatos

Document title	Predictive Assessment of dust production and fission product release for HTR-10
Author(s)	André Xhonneux (FZJ), Stephan Struth (FZJ), Claudia Druska (FZJ)
Number of pages	49
Document type	Deliverable
Work Package	WP 23
Document number	D23.11
Issued by	FZJ
Date of completion	30/01/2015
Dissemination level	Confidential, only for members of the consortium (including the Commission Services).

Summary

This document contains a description of the running-in phase of the HTR-10 modelled by VSOP and full core fission product release calculations with STACY.

Approval

Date	By
30/01/2015	Norbert KOHTZ
30/01/2015	Norbert KOHTZ
31/01/2015	Steven KNOL

Distribution list

Name	Organisation	Comments
P. Manolatos	EC DG RTD	Through the EC participant portal
All beneficiaries	ARCHER	Through the private online workspace

Table of contents

1 Introduction 4
2 VSOP model of the running-in phase 5
2.1 Calibration of control rods 5
2.2 Operation history 6
2.3 Fluid dynamics 7
2.4 Fuel shuffling 9
2.5 Results 16
3 SERPENT 17
3.1 HTR-10 model 17
3.2. Control rod worth: comparison with VSOP 17
4 STACY 19
4.1 Short description of the STACY code 19
4.1.1 Burnup calculation 19
4.1.2 Fuel shuffling model 22
4.1.3 Adaptation made to simulate running-in phases 24
4.2 Fission product release calculations of HTR-10 27
4.2.1 Description of main input values 27
4.2.2 FZJ calculations 30
5 Conclusions 48

1 Introduction

In the framework of an IAEA benchmark [1] in 2003 calculations with VSOP 99/05 were performed in Jülich to investigate the initial criticality of the HTR-10. The minimal filling level in the atmosphere of air that is needed for the first criticality was calculated. Within the CRP-5, temperatures were pre-defined (ambient temperature). For the work package a fluid mechanical input (THERMIX) and a shuffling scheme for the equilibrium core have been developed as presented in [2].

Now the simulation of the running-in phase up to the current state was done with VSOP 99/09 [3] to prepare the calculation of the fission product release.

Unfortunately, not all details regarding the current running-in phase are known. For this reason, the running-in phase being presented in this report is a possible running-in phase which takes the boundary conditions being published by INET [4] into account as far as possible. Boundary conditions for which any data could be found in literature have been resolved by reasonable assumptions.

The 10 MW_{th} pebble bed Helium cooled high temperature reactor, called HTR-10, has been built in the Institute of Nuclear Energy Technology of Tsinghua University. Spherical fuel elements with 60 mm in diameter with coated particles are used and the reactor contains about 27,000 fuel elements in the equilibrium core. Table 1 gives an overview of some main geometrical data and operation parameters at fuel load and Table 2 shows some characteristic values of the fuel element design.

Table 1 : Geometry and parameters at full load

Core diameter	150.0 cm
Average core height	197.0 cm
Number of control rods	10
Thermal power	10 MW
Helium mass flow	4.3 kg/s
Helium inlet temperature	250°C
Helium outlet temperature	700°C

Table 2 : Design of fuel elements within the initial core / equilibrium core

	In cylindrical core volume	In cone volume	Core average (being calculated)
Fuel fraction	57 %	0 %	51 %
Dummy fraction	43 %	100 %	49 %
Heavy metal content		5 g/sphere	
U235-Enrichment		17.0 w.-%	
Number of coated particles per Sphere		8300	
Number of fuel elements		27,000	
Average number of core passes		5	
Average burn up		80,000 MWd/t_{HM}	
Average power density		2 MW/m^3	
Average residence time		1080 d	

2 VSOP model of the running-in phase

To calculate the running-in phase of the HTR-10 the following technical aspects have to be adapted to existing VSOP model which has been used to predict the initial criticality:

- The rod worth profile specified in [5] needs to be reproduced in a preliminary VSOP calculation to enable the input for the burning-in phase.
- The power history given in [4] has to be translated to an usable format.
- Plausible thermal hydraulic input data for the running-in phase have to be found.
- A fuel shuffling scheme has to be developed accounting the complex fuel element and dummy element behavior.

2.1 Calibration of control rods

The VSOP model being used within this work package is based on the mode being developed as a contribution to the CRP-5 [1]. Within the CRP-5, aspects such as the filling level at which the first criticality is attained under air atmosphere are being studied. Due to the fact that the control rods were completely withdrawn during this experiment, the control rods were not being modelled**.** For the running–in phase the control rod worth is necessary to calculate the different power levels inclusive the zero power phases. As a first step, these rods have been modelled and calibrated. In case that the core geometry is modelled including the reflector cone, VSOP is limited to two dimensional calculations and three dimensional options cannot be chosen, because this case is limited to a description of the core in Cartesian coordinates. Due to this limitation of the model, the 10 control rods cannot be modelled individually in the model. Instead the well-known “grey curtain approach” is applied. The control rods need to be calibrated in the two dimensional model in such way, that the effect of a control rod movement is equal to a detailed description of the rods. Fig. 1 shows the results of the VSOP calculations with the calibrated rod worth.

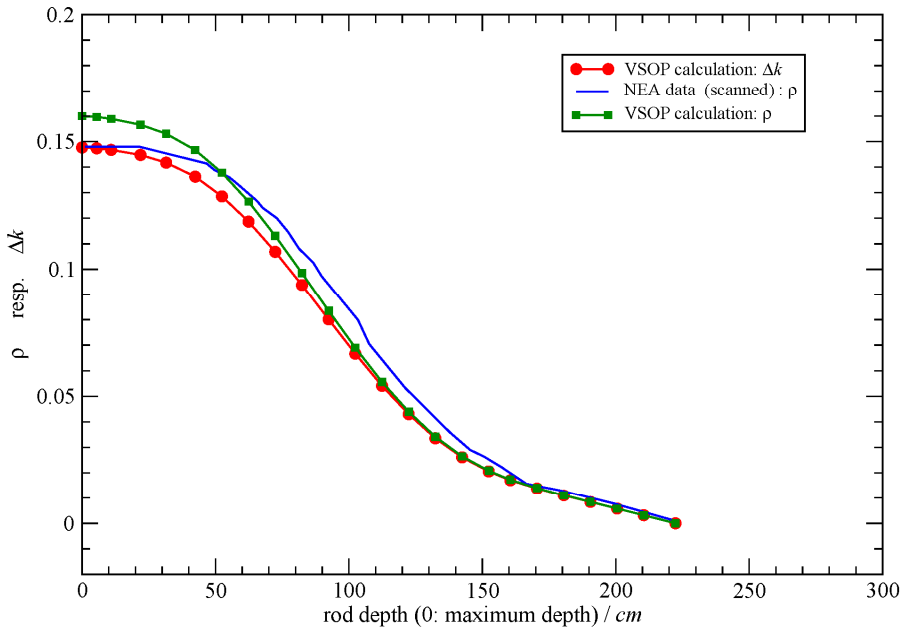

Fig. 1: Comparison of control rod worth

Since it is not certain whether the information in the NEA data refer on $\rho = \frac{\Delta k}{k}$ or $\rho = \Delta k$ both versions are given here. The VSOP calculation is based on $\rho = \Delta k = 14.7\%$.

2.2 Operation history

The HTR-10, being operated at INET at the Tsinghua University in Beijing is a test reactor with a nominal power of 10 MW_{th}. Many tests have been conducted to demonstrate different safety aspects of HTR. The first criticality was achieved on December 1, 2000 [6]. The reactor was operated at different power levels for different periods of time including many shutdown phases. The precise operating history has not been published. Nevertheless, Table 3 contains the year-averaged energies and a coarse power function has been published (see Fig. 2). Fig. 2 has been digitalized in a first step. In a second step the resulting curve has been condensed to form a power histogram, containing time steps with a constant power level (see Fig. 3).

Table 3: Table of performance history (the data of the left four columns are taken from [4])

Year	Operation days [d]	Average work [MWd]	Average power [MW]	EFPD [d]
2003	106	258.9	2.44	25.89
2004	168	708.5	4.22	70.85
2005	149	821.4	5.51	82.14
2006	97	532.0	5.48	53.20
2007	49	182.6	3.73	18.26
total	569	2503.4	21.38	250.34

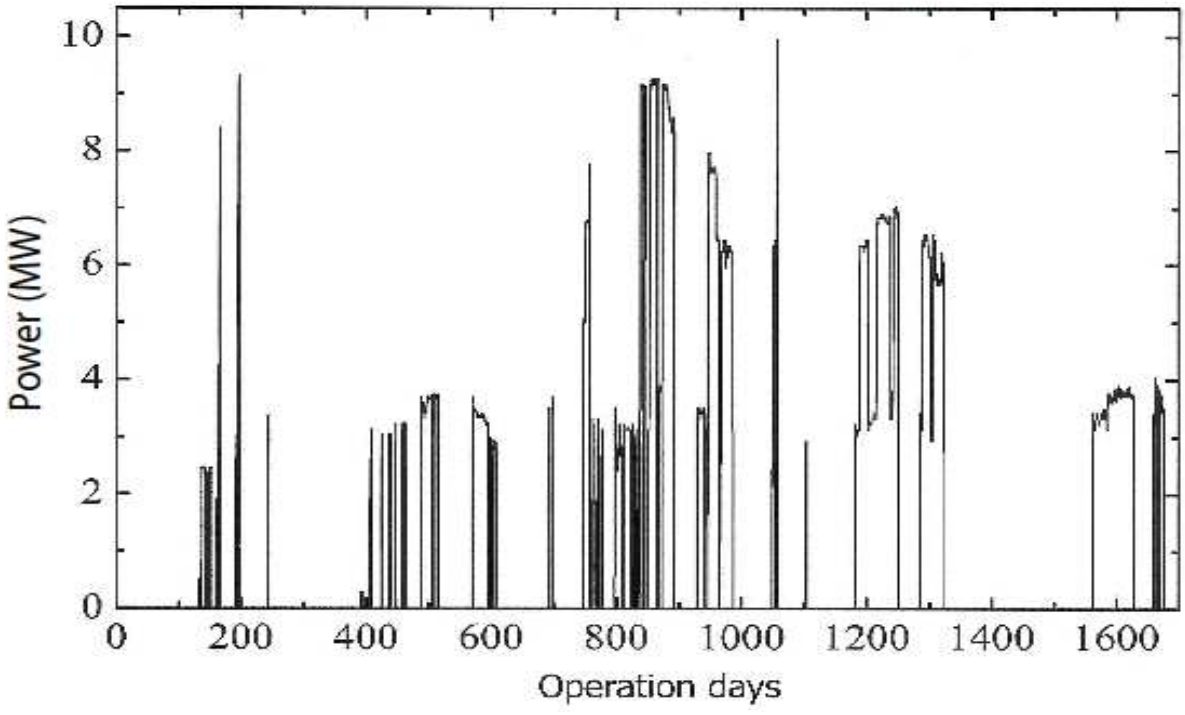

Fig. 2: Power histogram of HTR-10 [4]

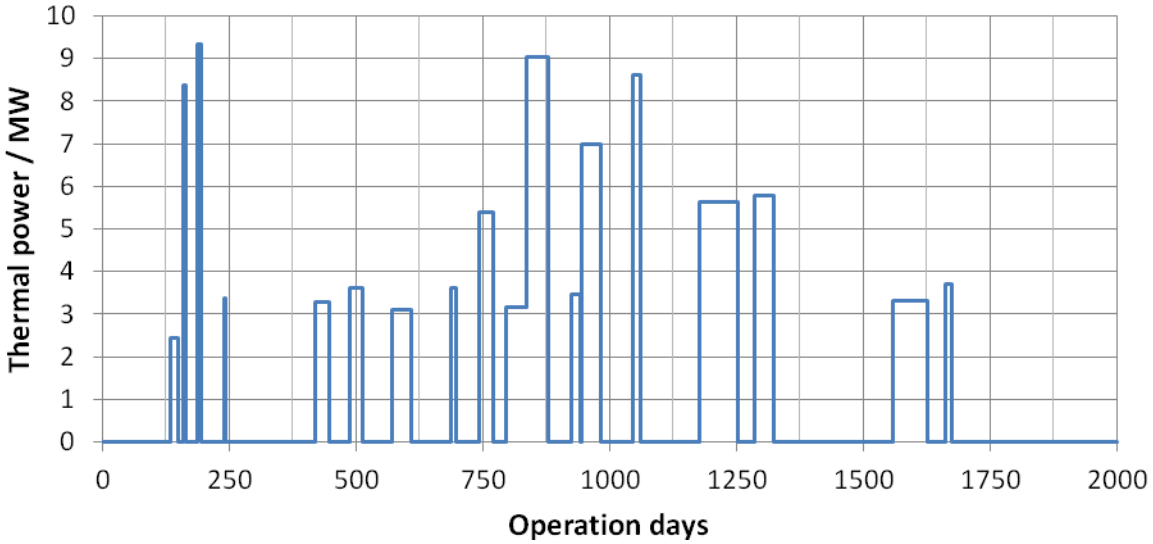

Fig. 3: Power histogram of HTR-10 (based on Fig. 2)

As an example Table 4 shows the first 14 time steps. The data were read from Fig. 3 and were used by VSOP to simulate the running-in phase. One of the key parameters influencing the reactivity of the core is the fuel shuffling rate. This rate can be set by the frequency at which the content of the regions is being shuffled. This frequency is set by defining the time in between two shuffling steps ("DELDAY", see 4th column in Table 4).

Table 4 : Data used by VSOP extracted from the power history (see Fig. 3)

No.	Power [MW]	Time [d]	DELDAY [d]	Control rod position [cm]	Mass flow [kg/s]	Inlet temperature [°C]
1	2.4465	16	4.0	265.9	0.942	200
2	0	10	5.0	394.2	-	-
3	8.3792	6	3.0	261.7	3.584	250
4	0	23	11.5	394.2	-	-
5	9.3272	7	3.5	261.7	3.99	250
6	0	45	22.5	394.2	-	-
7	3.3639	3	1.5	261.7	1.349	220
8	0	176	88.0	394.2	-	-
9	3.2756	9	4.5	261.7	1.314	220
10	0	41	20.5	394.2	-	-
11	3.6086	26	4.33	261.7	1.447	220
12	0	58	29.0	394.2	-	-
13	3.1083	39	4.875	261.7	1.247	220
14	0	78	39.0	394.2	-	-

2.3 Fluid dynamics

To simulate the different power levels as shown in Fig. 3 and Table 4, the flow rate and the coolant inlet temperature have to be varied. They are functions of the power level at which the reactor is being operated (part-load diagram), and be needed for the fluid dynamics calculations with THERMIX. Due to the many similarities between the HTR-Module and the HTR-10, it has been assumed that the part-load diagram of the HTR-Module is (at least) similar to the one of the HTR-10 (as detailed boundary conditions are not published for the HTR-10). For this reason, the part-load diagram of the HTR-Module [7] has been used to set the missing parameters of the fluid dynamics calculations (see Fig. 4).

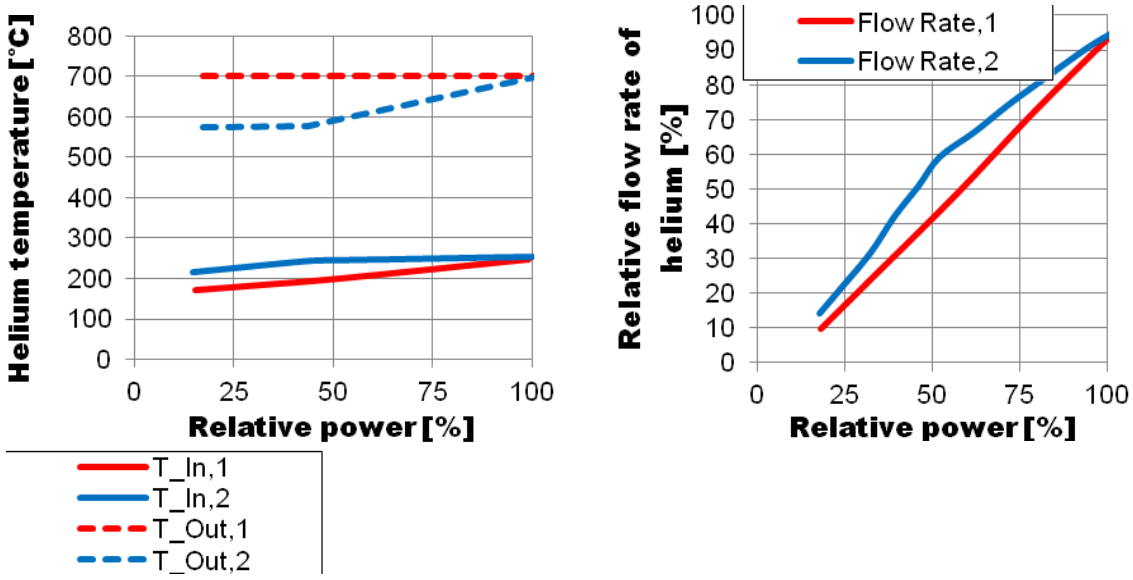

Fig. 4: Part-load diagram of HTR-Module [7]

The part-load diagram of the HTR-Module is not a single curve but defines limits, between which the reactor can be operated. It can be seen, that the flow rate of the coolant is varied almost linearly with the power level. [8] states, that in principal the HTR-Module can be operated between a partial load level of 20 % and full load, but there are some limitations. A full Xenon override can only be achieved for 10-50-100 % load changes. Load changes to 20-50 % depend on the actual Xenon inventory. For even lower power levels, other actions have to be taken. Fig. 5 shows the Helium inlet temperature and the Helium flow rate for the HTR-10 model of VSOP.

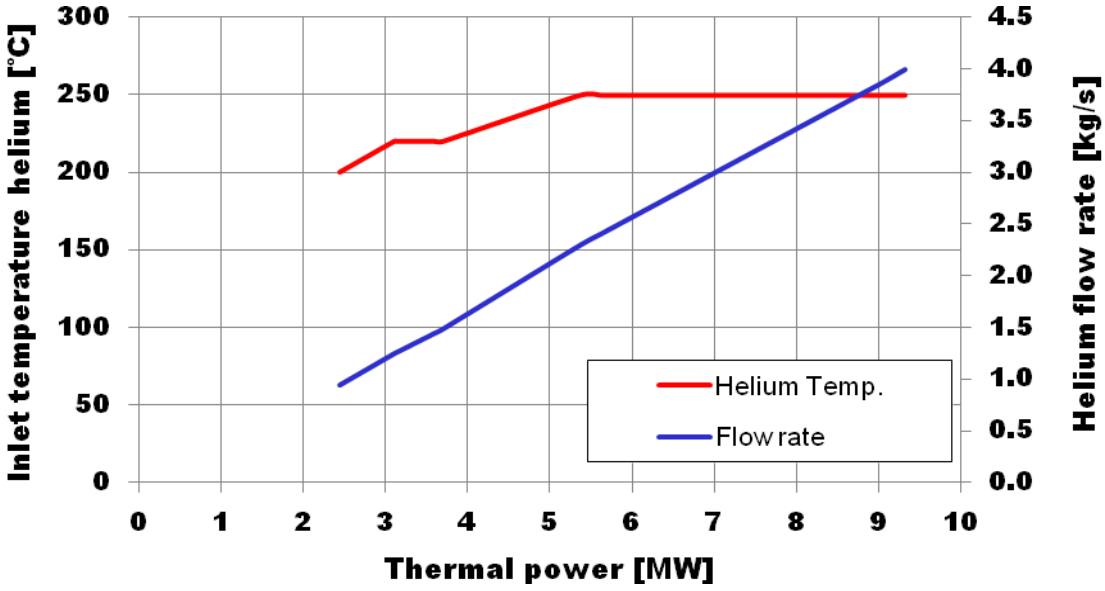

Fig. 5: Helium inlet temperature and flow rate as a function of the power level in the VSOP model of HTR-10

Within the calculation performed by FZJ, no coolant flow was assumed in the discharge chute. A paper published by INET assumed a bypass flow of about 1-2 % of the total flow rate [9]. Due to this, the temperature profile in the lower part of the core unveils a different shape in both studies. Both the temperature curve of the surface and the central fuel element temperatures are almost identical for both studies in case of the equilibrium core (see Fig. 6).

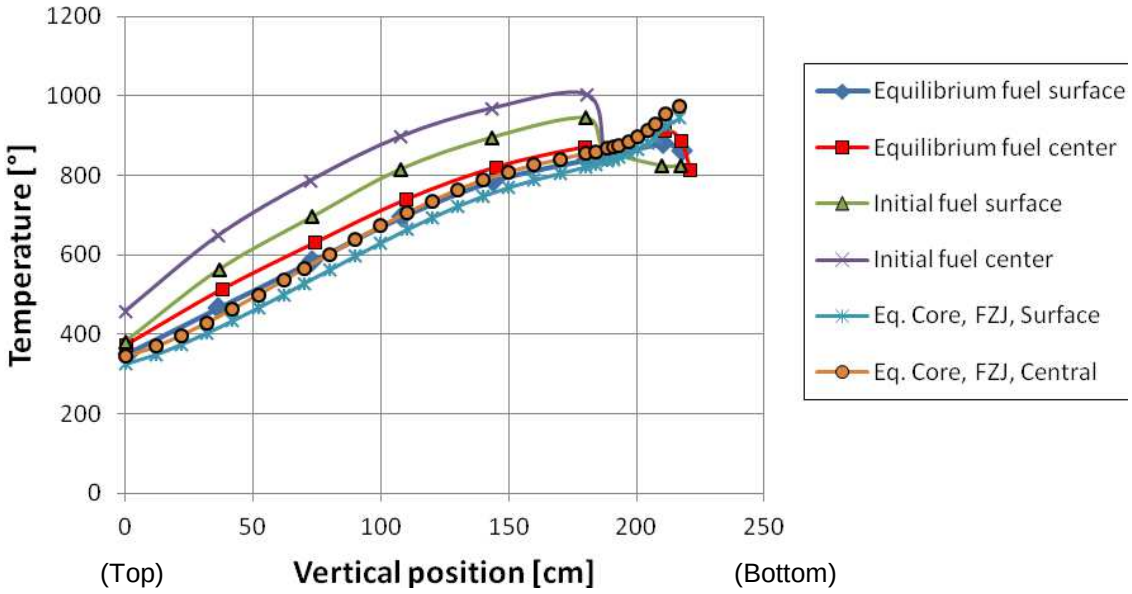

Fig. 6: Fuel surface and center temperatures for both the equilibrium core and the initial core

In the analysis, the gas flow through the reactor core is chosen to be 86 % of the rated flow [9]. It is conservatively assumed that 14 % rated flow passes through the control rods, fuel discharge tube and gaps between graphite components [9]. In reality, the bypass flow can be reduced to less than 10 % of the total flow [9].

2.4 Fuel shuffling

As a part of the VSOP model, for different constellation of fuel and dummy elements a spectrum cell is being modelled. In case of the HTR-10 model, four different spectrum cells are needed:

- A spectrum cell containing solely dummy elements
- A spectrum cell containing the initial mixture of fuel and dummy elements
- A spectrum cell containing solely fuel elements
- A spectrum cell for the reflector area.

One of the above mentioned spectrum cells is assigned to each of the spectrum zones. In addition to the fuel shuffling scheme, which needs to be defined to model the fuel management as close as possible to the chosen way of operation for the HTR-10, the assignment of the spectrum cells needs to be readapted at the end of each fuel shuffling step. This is needed because the content of at least one region is altered as long as dummy elements are part of the pebble bed. In case of the equilibrium core, only two (solely fuel and reflector area) of the initial four spectrum cells are needed.

In [10] the ideal running-in phase without any shutdown phases is regarded. Induced by the relative low height to diameter ratio of the HTR-10 core, the flow pattern cannot be modelled as a cylinder where pebbles at different radii move with equal velocity through the core. The flow velocity can be adapted in VSOP by the following procedure. The pebble flow is modelled according to the stream tube model. For this reason, the pebble bed is divided in so-called channels (stream tubes), which are limited by flow curves and or a reflector surface in the radial direction. Each of these channels is subdivided in regions of equal volume. The continuous pebble flow is being approximated by a step-wise moving of the complete content of a region to the region below. Thus, the number of regions per channel influences the speed with which fuel flows through a channel. Each of the regions contains in general one or several batches, where each batch represents a specific fuel type at a specific (burnup) state. For each region belonging to the same channel, the number of batches is equal. Batches have no distinct position within a region; they are being treated as a homogenous mixture.

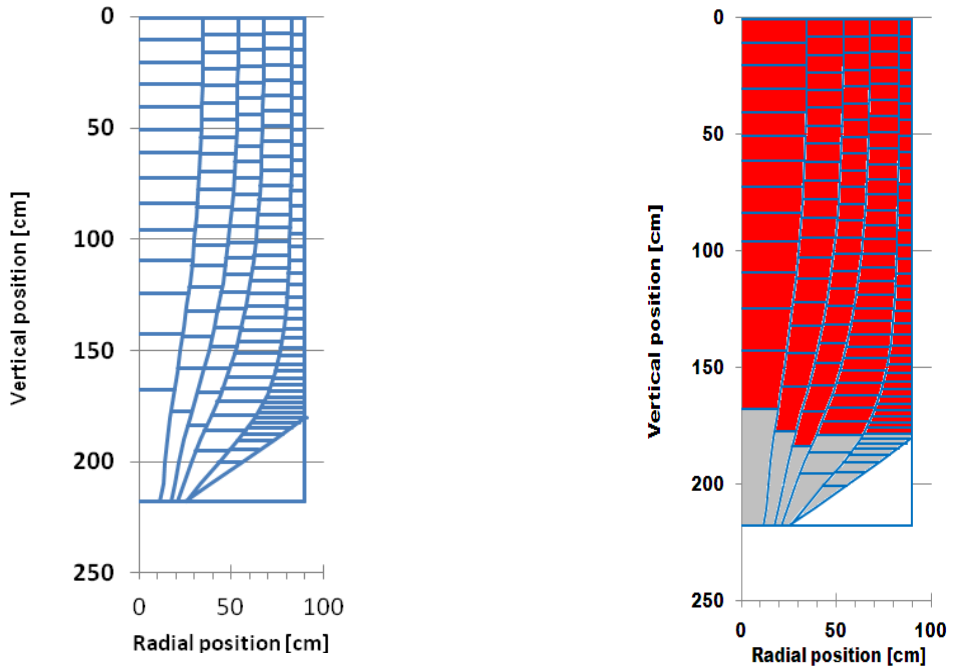

Fig. 7: a) Fuel channels, divided into regions of equal volume in case of HTR-10
b) Initial loading of core (red: mixture of fuel and dummy elements, grey: 100% dummy elements)

Compared to [10], the number of regions per channel has been doubled to (14/20/24/32/42 regions in channel 1, 2, 3, 4 and 5 respectively), in order to improve the approximation of the boundary between the cylindrical core volume containing a mixture of fuel (57 %) and dummy elements (43 %) and the hopper zone. This hopper zone contains solely dummy elements (see Fig. 7).

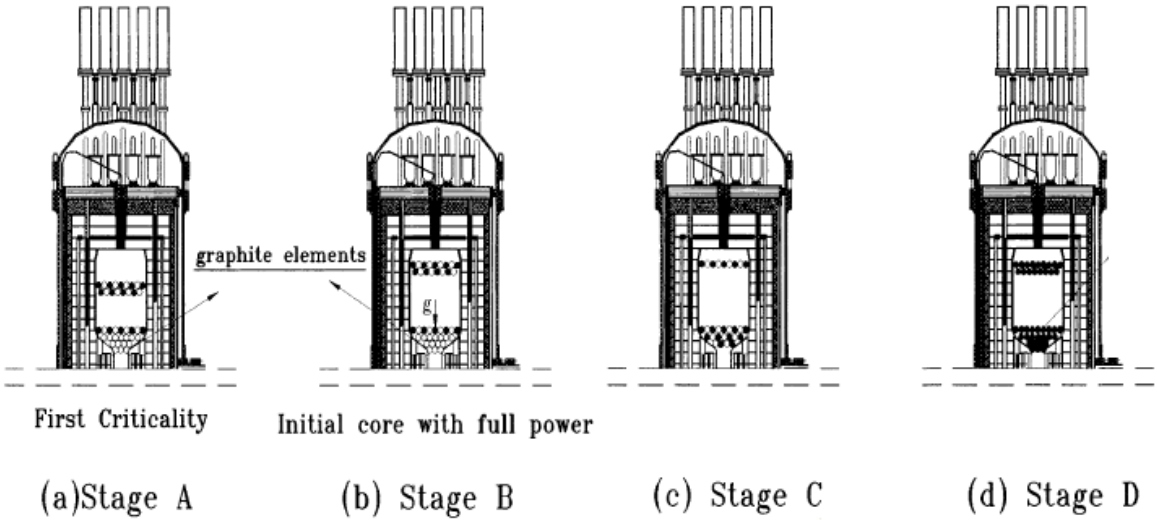

Fig. 8: Different stages during running-in phase of HTR-10 [10]

Reference [10] describes in detail the procedure being followed to execute the running-in phase. The following section provides an overview of the information being extracted, deduced and used a general assumption being made to model the running-in phase in VSOP 99/09.

1) The initial core which is completely filled contains excess reactivity. It is possible to operate the reactor without shuffling the core by means of adding fresh fuel to the core for several days (see stage B in Fig. 8).

2) After this, it is needed to shuffle the core to maintain the core being critical. Meanwhile, spheres are discharged from the lower part of the core. During the first fuel shuffling steps, the regions being discharged contain batches with dummy elements only. As long as only dummy fuel elements are being discharged, a mixture of fuel and dummy elements (the same mixture as the one being present in the cylindrical part of the initial core) is added to the upper end of the core (see Stage C in Fig. 8). As soon as the batches containing fuel elements are being discharged, only fuel elements are added to the core (see Stage D in Fig. 8). These can be recycled fuel elements from the lower part of the core or fresh fuel elements. Due to this, the fraction of dummy elements is being lowered gradually from this time during the running-in phase, see Fig. 9. This curve can be deduced from the fuel shuffling scheme analytically. After 43 fuel shuffling steps, all batches containing dummy elements have been discharged from the core and are scrapped. Meanwhile, fuel elements are recycled during and not scrapped during these shuffling steps. From this moment, only batches containing fuel elements are within the core. Meanwhile, the fraction of recycled fuel elements to the total number of elements added to the upper end of the core increases, because all fuel is being recycled (at least up to 4 core passes!). Therefore, the number of fresh fuel elements to be added to the core decreases during this period. From the time point where fuel is scrapped and not recycled because the burn up limit of 72,000 MWd/t_{HM} is achieved, the fraction of fresh fuel elements increasing again up to the fraction of 25 % in case of the equilibrium core.

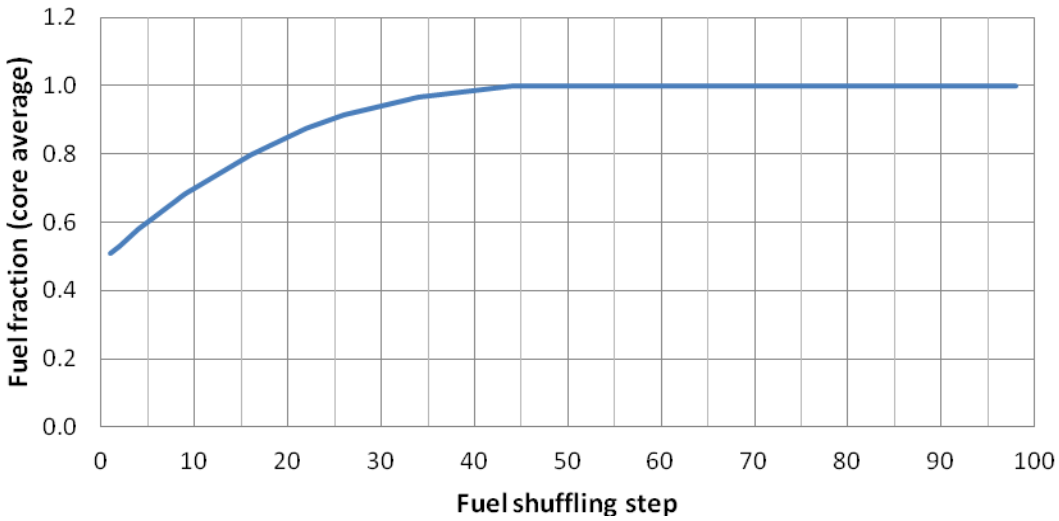

Fig. 9: Fuel fraction in the HTR-10 core during the running-in phase

3) In general, movements at the upper and lower end of the core are user defined in case of a pebble bed reactor. The movement between the other regions is performed automatically. These user defined actions define which batch has to be moved from and to which position. Normally, in case of an equilibrium core being operating as a multi fuel pass reactor, a batch is being shuffled a distinct number of times before being scrapped. In reality, the precise number of core passes is not known, because the elements are not tagged / marked. Instead, the current burn up is being measured and the fuel elements is being recycled or scrapped according to the burn up attained. According to the paper, fuel is being recycled as long as the burn up does not exceed 72,000 MWd/t_{HM}. The fuel elements are designed to achieve an average burn up of 80,000 MWd/t_{HM}. Nevertheless, some fuel elements will attain a higher burn up, due to the fact that the average power exceeds the average power per fuel elements in the equilibrium core. The fuel elements can withstand higher burn up levels but should not exceed a burn up of 100,000 MWd/t_{HM} [10]. A further increase could result in higher pressures within the coated particle which could lead to an increase of the coated particle failure fraction and consequently higher fission product release.

Due to this, the running-in phase could only be calculated step-wise from the time point where fuel is discharged which has passed the core for the fourth time. Depending on the burn up attained, fuel is

being moved to a so-called fuel shuffling box (which can be moved to the top of the core during the next fuel shuffling step) or is scrapped.

4) In general, properties (like for example the nuclide vector) of the batches being moved to the same fuel shuffling box are being homogenized before the resulting batch can be reintroduced to the core. For the HTR-10 model, in case that batches are moved to a fuel shuffling box, batches with an identical core pass number are being collected in one individual box, because these batches represent spheres with a similar burn up state.

5) One of the key parameters influencing the reactivity of the core is the fuel shuffling rate. This rate can be set by the frequency at which the content of the regions is being shuffled. This frequency is set by defining the time in between two shuffling steps (VSOP variable “DELDAY”). Normally, these time step widths have to be determined iteratively by simulating a new running-in phase. Because this process has already been performed by INET, this process can be sped up by using the time step width resulting from these calculations. Nevertheless, some minor differences can occur between the time step width being determined by INET and the simulation being presented in this report, due to the fact that some (minor) differences can exist between some assumptions being made.

   The rate at which fuel is added to the core is given as a continuous function. This continuous rate can be retransformed into values of “DELDAY”. During each fuel shuffling step, the volume of each most upper region has to be refilled again, to maintain a constant filling level of the core. For this reason, an average of 1,043.76 spheres has to be added to the top of the HTR-10 core during each fuel shuffling time step, assuming an average filling factor of 61 % of the spheres in the core volume.

Table 5: Geometry of channel and regions resulting in number of spheres shuffled per fuel shuffling step

Channel-ID	Total volume of channel [cm^3]	Number of regions	Region volume (solid + void) [cm^3]	[Spheres/region]
1	5.198400E+05	14	37,134.1	200.29
2	8.095500E+05	20	40,480.0	218.33
3	9.044800E+05	24	37,687.9	203.27
4	1.640500E+06	32	51,263.0	276.49
5	1.143100E+06	42	26,953.1	145.37
Sum	**5.017470E+06**	**132**	**Sum (spheres/shuffling step)**	**1043.76**

This enables to re-transform the continuous shuffling rate into a set of times between shuffling steps (see Fig. 10), which can serve as a main indicator for the VSOP simulation. It can be seen, that the time between two fuel shuffling steps is relatively high due to the excess reactivity of the core at the beginning. Fresh fuel needs to be added at a low rate to maintain the core critical. Up to some certain time step, all fuel elements being discharged are being recycled, resulting in an increasing level of depletion of the fuel. For this reason, it is necessary to shuffle the pebble bed at a higher pace to add fresh fuel elements to the core. With increasing time, the slope of the histogram displaying the time between two fuel shuffling rates decreases, as one indicator that the core is nearing the equilibrium state.

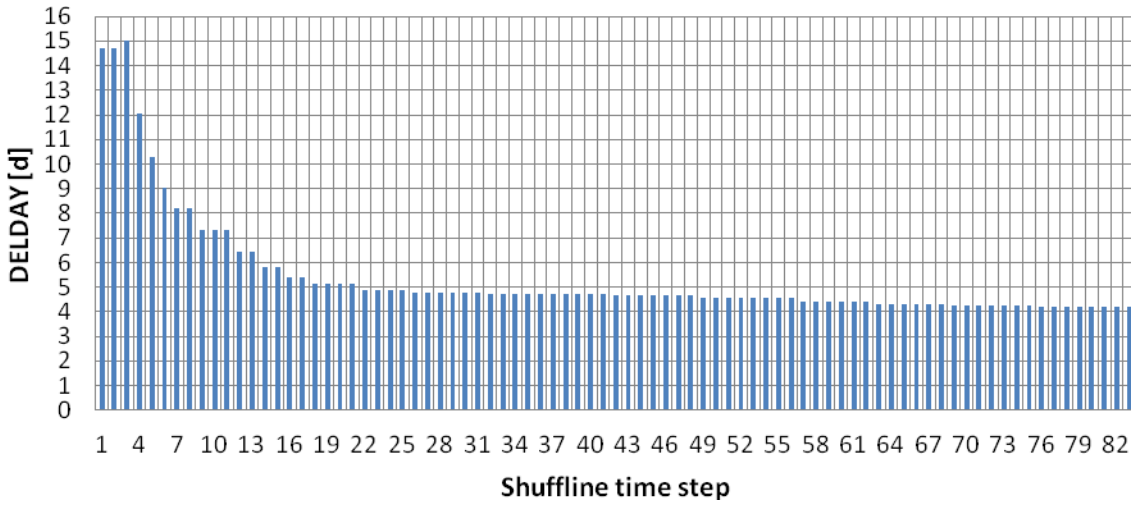

Fig. 10: HTR-10 Shuffling time step width during running-in phase at full power (10 MW)

Due to the fact that each channel has a channel specific number of regions, the fuel shuffling schemes are irregular. From the initial core to the fuel shuffling scheme being used for the equilibrium core, 90 individual fuel shuffling schemes are needed. These fuel shuffling schemes take into account that different kinds of batches (containing dummy or fuel elements) or fuel elements with different core pass numbers are unloaded from the lowest region of different channels at the end of different fuel shuffling steps. An example of such a fuel shuffling scheme is being displayed in Fig. 11 schematically. The fractions of the different burn up levels of the fuel are equal for all regions of all fuel channels.

As mentioned before, the core is divided in 5 channels, where each channel has its specific number of regions (14/20/24/32/42). The colours in the rectangular boxes, which represent the batches, illustrate the type of the batch (fuel or dummy element) and the core pass number. Due to the fact that no dummy elements are recycled, all dummy elements have core pass number 1. The numbers at the very lower and upper end in the figure illustrate from which box number fuel is moved to the core (upper end of the core) and to which box is being moved (lower end of the core). This figure illustrates clearly the irregular fuel shuffling which occurs due to the different region numbers in the channels. Although the most two inner fuel channels (left) contain fuel which are about to finish their third core pass, the most outer fuel channel (right) contains still dummy elements within the lower part.

The fuel shuffling scheme of the equilibrium core is displayed in Fig. 12. As soon as each region of each fuel channel contains fuel elements with core pass numbers ranging from 1 to 5, the same fuel shuffling scheme can be applied.

The HTR-10 core has been operated for about 250 EFPD (see Table 3). It is clear that the equilibrium has not been reached at this point, but rather will be reached after a multiple of the current operating time.

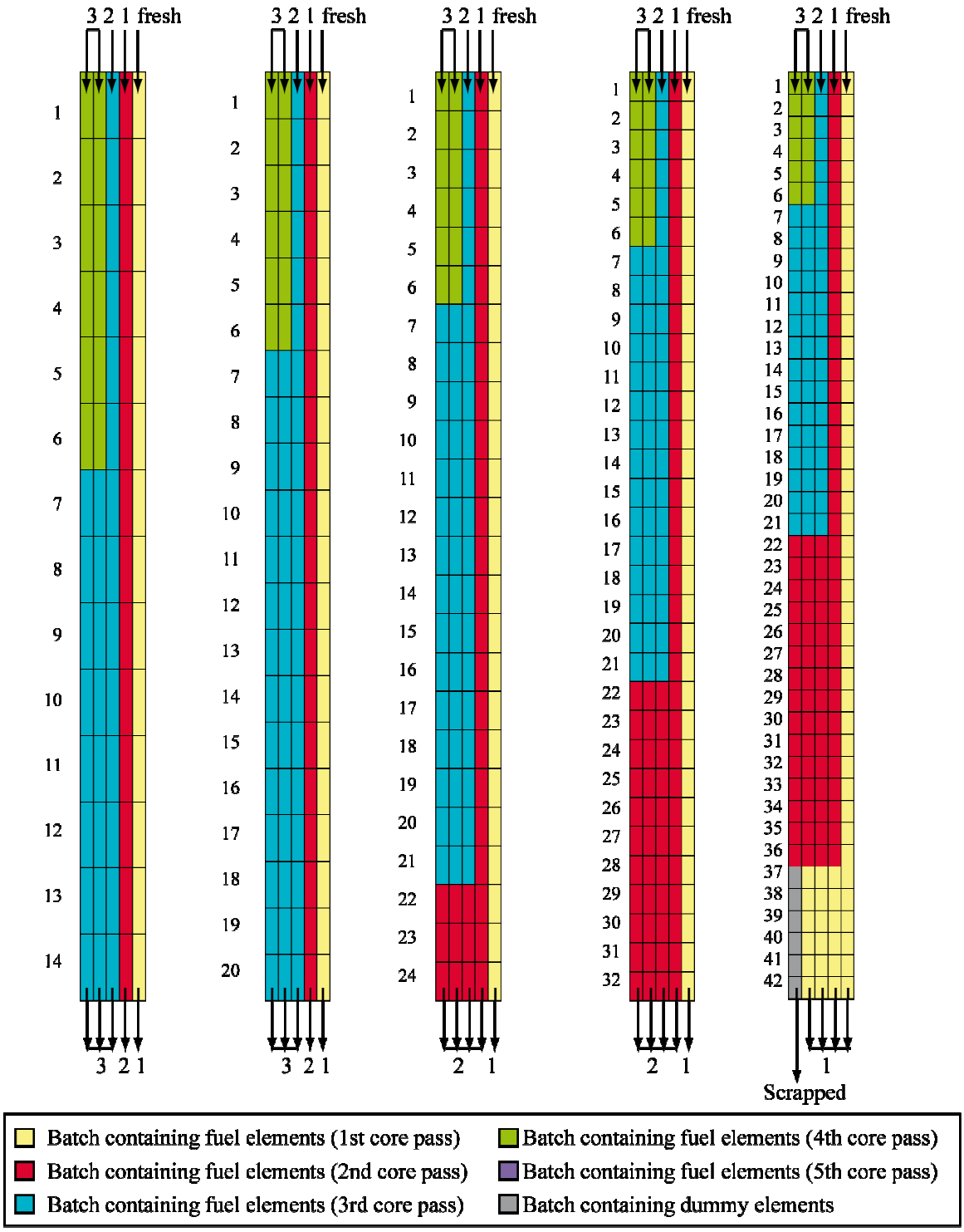

Fig. 11: Exemplary fuel shuffling scheme during the running-in phase of HTR-10 demonstrating the core content at a specific time point and all movements crossing the core boundary at the upper and lower end of the pebble bed

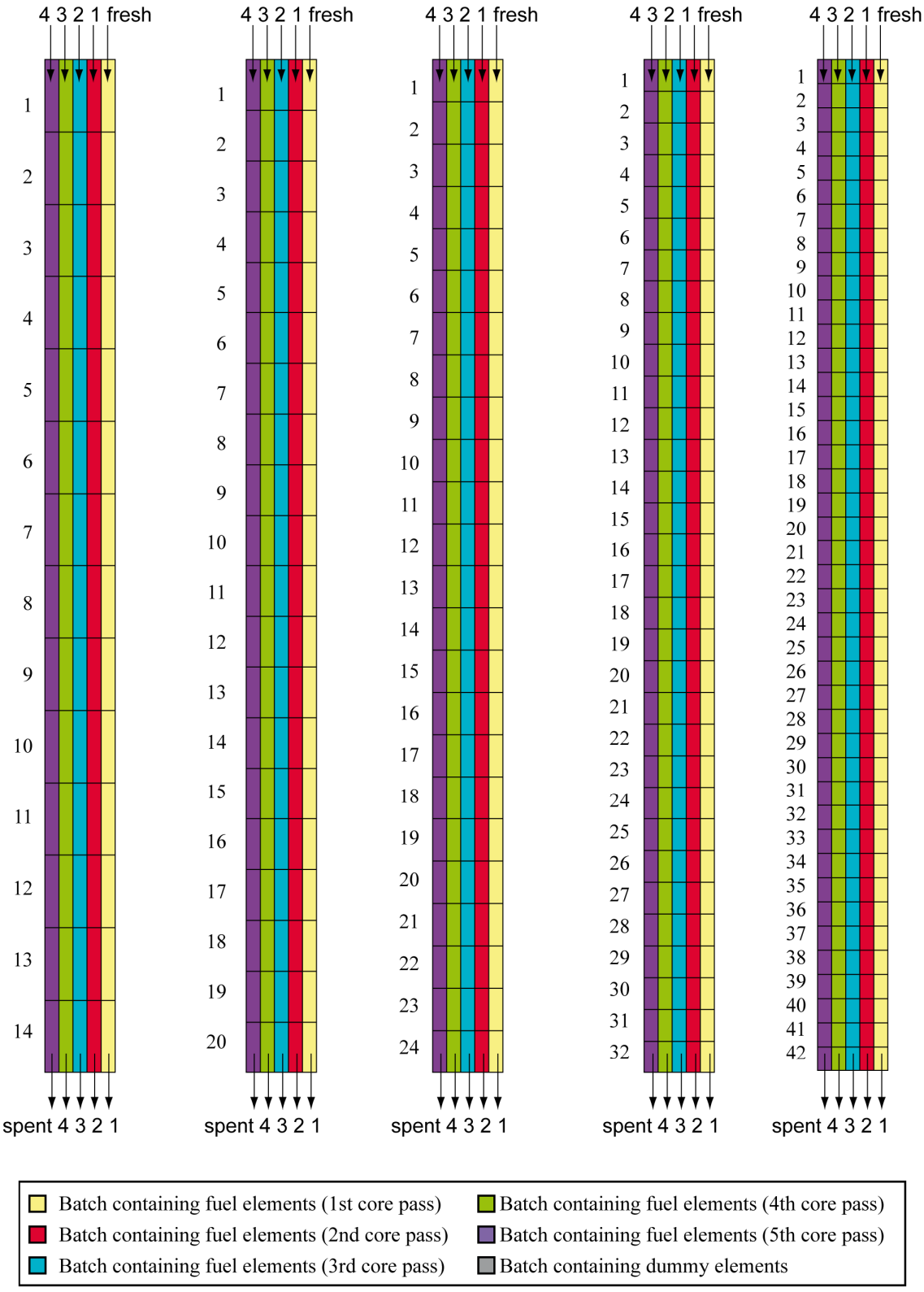

Fig. 12: Fuel shuffling scheme demonstrating the core content of the equilibrium and all movements crossing the core boundary at the upper and lower end of the pebble bed

2.5 Results

For a given fuel element configuration and a given core loading the multiplication factor k_{eff} is determined only by the position of the control rods and the shuffling frequency of the fuel. Both values can be used in VSOP only in a discrete form. The variable “DELDAY” describes a large time step in which the fuel is circulated twice. In a continuously operating reactor k_{eff} (control rods in constant position) can be set precisely by varying “DELDAY”. In the case of real running-in of the HTR-10 there are many different power levels including zero loads. So “DELDAY” has to be adjusted to the given time frame (operating time of a block divided by integer = DELDAY, see Fig. 3 and Table 4). An exact adjustment on $k_{eff} = 1{,}0$ is not possible. A technical alternative to compensate would be possible by moving the control rods. This approach, however, does not reflect reality, as it merely a problem of numerical discretization would be corrected. Therefore, the control rods are not moved. However Fig. 13 shows that all values of k_{eff} calculated by VSOP account within the control range of the rods.

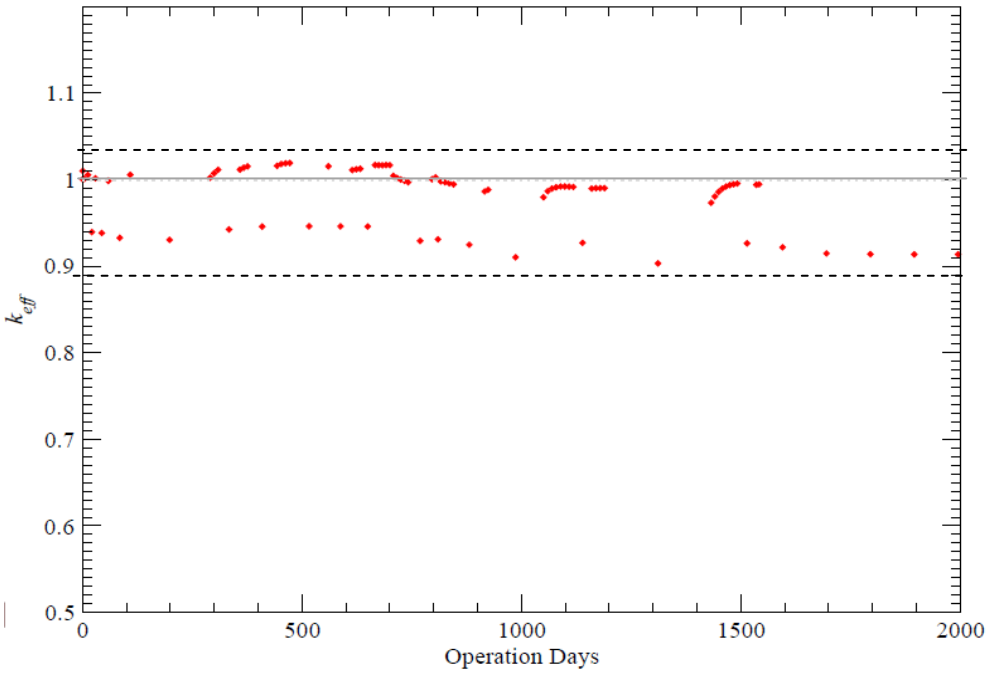

Fig. 13 : Calculated reactivity values from VSOP during operation and zero load

The multiplication factor k_{eff} is between 0.9 and 0.95 during zero load phases while the control rod position is 394.2 cm. The fully withdrawn position of the rods is 171.7 cm measured from the top of the boronated carbon bricks

It needs to be assured that the reactor can be shut down during all time steps of the running-in phase. The core is being fuelled with one type of fuel elements, which means that the fuel type forming the equilibrium core is being part of the initial core as well. The fuel is blended down by adding dummy elements. Due to the fact that the number of fuel elements is rather low during the first time steps, the demanded power is generated by fewer fuel elements than in case of the equilibrium core. The average power per sphere decreases with time. In the equilibrium core the average power production is equal to 0.53 kW/sphere. Induced by these higher powers, fuel temperatures are higher during the running-in phase which is a factor which needs to be looked at.

3 SERPENT

3.1 HTR-10 model

Comparisons have been conducted with a Serpent Model of the HTR-10. Serpent is a Monte-Carlo neutronics code including burn up calculation which has been developed by the VTT Technical Research Center in Finland [11]. Control rod worth values have been determined for the HTR-10 completely filled up with the mixture of fuel and dummy elements under helium atmosphere at operating pressure. Within the Serpent model, the Spheres are placed according to a regular lattice. By using a Monte-Carlo method, it is being determined which sphere contains fuel and which does not. It is checked whether the average filling factor of 61 % and the fuel fractions in both zones are achieved. In comparison to the VSOP model, the fuel pile at the upper end of the pebble bed is being modelled with an inclination of 20 degrees (see Fig. 14).

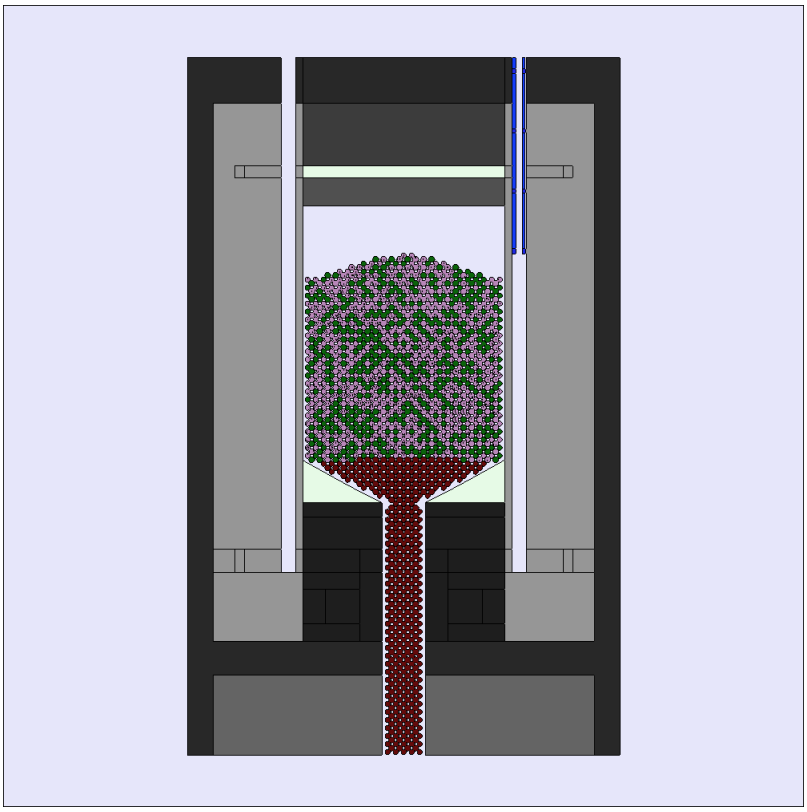

Fig. 14: The HTR-10 core in the Serpent model

3.2. Control rod worth: comparison with VSOP

To compare the SERPENT model with the VSOP rod worth calculation all ten rods are simultaneously and fully inserted. The reactivity respectively Δk results from the simulation in the fully inserted case are

$$\rho = 0.1709 \pm 0.0008 \qquad \Delta k = 0.1490 \pm 0.0006 \ .$$

The results calculated with VSOP are

$$\rho = 0.159974 \qquad \Delta k = 0.14766 \ .$$

The deviations are about 7 % (reactivity) and about 1 % with respect to Δk . Fig. 15 shows the process of reactivity during insertion of all control rods.

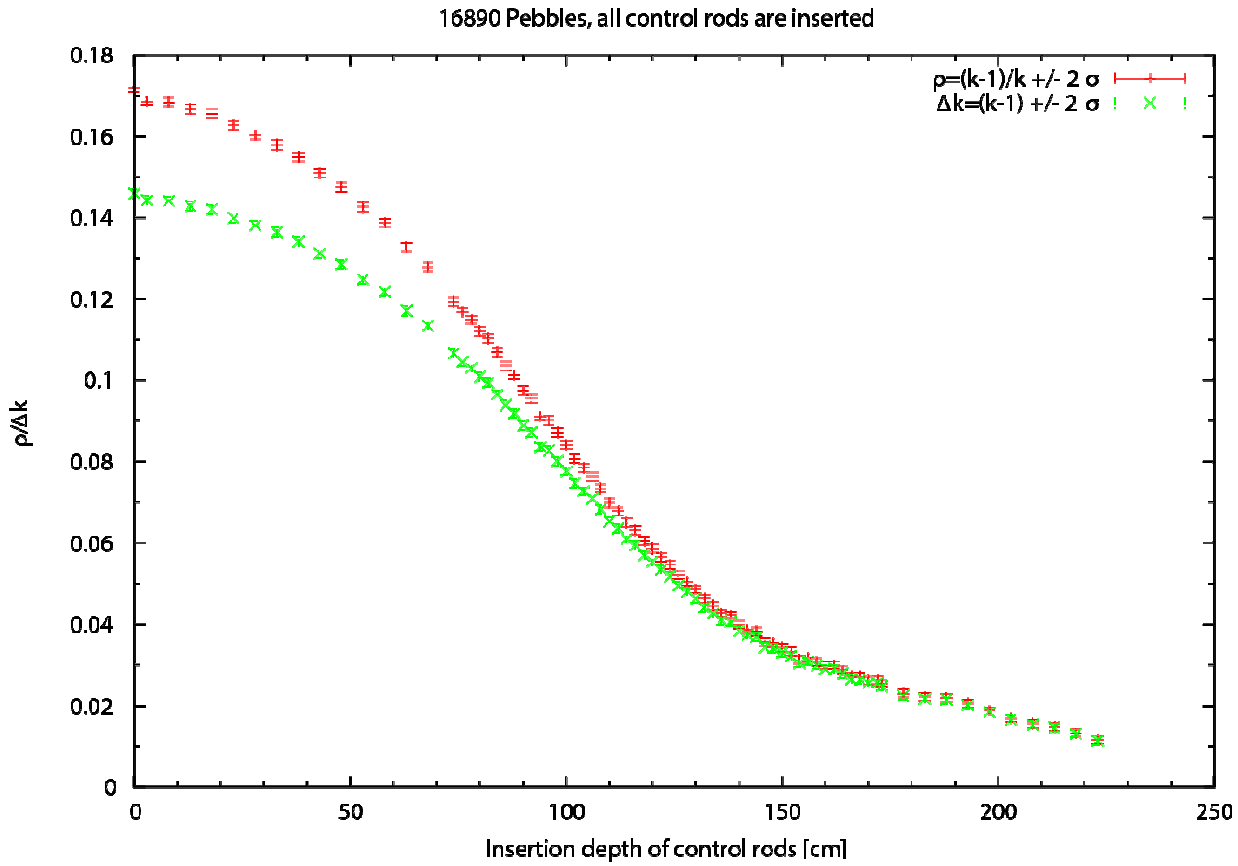

Fig. 15 : Process of reactivity during insertion of all control rods

4 STACY

4.1 Short description of the STACY code

The fission product release rates of some nuclides which are of radiological importance have been calculated by using the Source Term Analysis Code sYstem (STACY). First of all, STACY will be introduced and important improvement made in comparison to its predecessor FRESCO-II will be discussed.

The version of STACY which has been developed within the framework of a PhD study is able to calculate the fission product release rates for an equilibrium core and during transients starting from this equilibrium core [15]. In this case, the fission product release rate is being determined by simulating the release rates of a large number of individual, so called “tracer pebbles”. Great care is taken to position these tracer elements in such way, that the fission product release rates of these spheres are representative for the complete pebble bed.

With the STACY computer model, predictive calculations have been performed for the HTR-Module. These results have been compared to former results being determined by Siemens Interatom. For example for the DLOFC accident, it could be shown, that the fission product release rate of the short-lived nuclide I-131 is higher due and those of long-lived nuclides are lower according to STACY simulation in comparison to values determined by Interatom. The burnup calculation has a major influence on the I-131 inventory, because the pebble’s inventory is fluctuating during each core pass, which was not taken into account by the simplified inventory calculation being used in FRESCO-II.

4.1.1 Burnup calculation

An important aspect of the fission product release calculation is the simulation of the nuclide inventory, which is treated in STACY in more detail. Different from FRESCO-II, STACY uses the newly implemented burnup core TNT (Topological Nuclide Transformation), which is comparable to the burnup code ORIGEN, to determine the time-depending inventory of the differing fission product of interest. FRESCO-II calculates fractional release and fractional release rates where the fission product release is related to the fuel element inventory at the end of the irradiation phase. The inventory between start and end of the irradiation phase is treated in a rudimentary way.

Neglecting several terms of the differential equation which describes the time dependent nuclide inventory N_{FP}, the time depending fission product inventory can be written as:

$$\frac{dN_{FP}}{dt} = \gamma_{FP} \cdot \sum f \cdot \phi - \lambda \cdot N_{FP}(t) - \sigma_A \cdot N_{FP}(t) \cdot \phi \qquad \text{(Eq. 1)}$$

Assuming a constant neutron flux Φ and an absorption cross section σ_A equal to zero, the time depending inventory can be calculated with the following equation:

$$N_{FP(T)} = Q_{FP} \frac{1 - \exp(-\lambda \cdot t)}{\lambda} + N_{FP,1} \cdot \exp(-\lambda \cdot t) \qquad \text{(Eq. 2)}$$

where: $N_{FP,1}$ / $N_{FP,2}$: Inventory of the fission product at the start and end, respectively, of the calculation / irradiation phase

Q_{FP}: Source term

In this equation, the increase of the fission product amount is considered by an imaginary source term. According to this equation, fission products disappear only due to decay.

Per definition, the inventory of the fission product at the start of the simulation ($N_{FP,1}$) is equal to zero, the inventory at the end of the irradiation phase is equal to one. The imaginary source term is constant during the irradiation phase (constant conditions) and is equal to zero (assuming no power excursion). The imaginary source term has to be set in such way that these boundary conditions are met. Thus, the time depending (relative) inventory in FRESCO-II is only a function of the decay constant of the nuclide of interest.

As an example, Fig. 16 shows the cesium 137 inventory as a function of time related to the inventory at the end of the irradiation time. The first three curves have been calculated with the TNT code, assuming different constant neutron fluxes (flux = 7.0x10^{13}, 1.0 x10^{13} and 1.0 x10^{12} n/(cm^2·s)). In addition the relative inventory according to the FRESCO-II approach has been displayed. With increasing level of the neutron flux, the difference between the burnup code and the simplified equation of FRESCO-II is increasing.

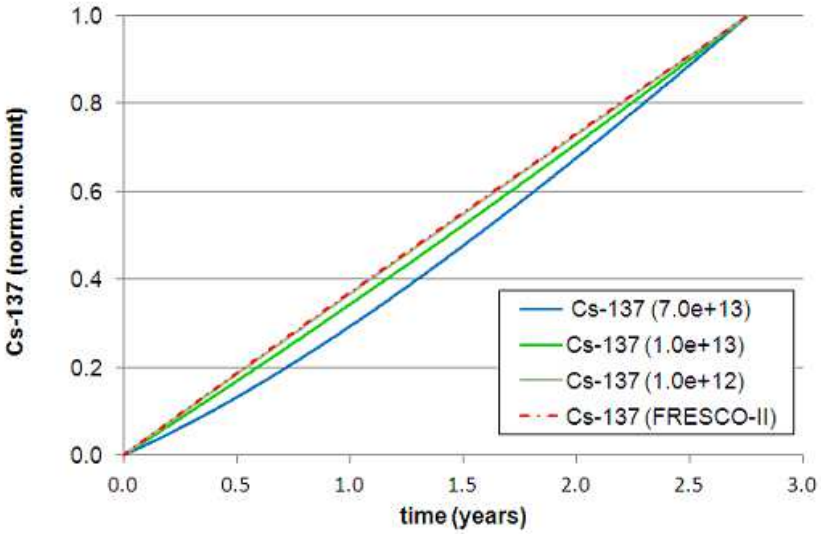

Fig. 16: Cesium 137 inventory as a function of time (TNT simulation)
Burnup of 92 mole U-238 and 8 mole U-235 (neutron flux in 1/cm^2/s)

To take the time depending inventory in the fission product release calculation into account, equation 2 has been extended. Instead of one constant source for the whole operating time, an imaginary source term is determined for each time interval using the inventory at the beginning and end of this interval. The following equation, which is comparable to equation 2, can be used for each interval:

$$N_{FP}(t) = \frac{\lambda}{1-\exp(-\lambda \cdot t_{NOC})} \cdot \left[N_{FP,2} - N_{FP,2} \cdot \exp(-\lambda \cdot t_{NOC})\right]\left(1 - \frac{\exp(-\lambda \cdot t)}{\lambda}\right) + N_{FP,1} \cdot \exp(-\lambda \cdot t)$$

(Eq. 3)

Fig. 17 shows an example for the application of this equation by using the HTR-Module as an example. Here, the cesium 137 inventory is displayed during the first core pass in fuel channel 1 (pebble flow along the symmetrical core axis). The inventory after the simplified equation used in FRESCO-II using 2 data points (inventory at start = 0, inventory at end = 1) is a straight curve due to the long half-life of the cesium isotope. The data points are generated by the ORIGEN calculation which can be started after having performed a VSOP calculation. The resulting ORIGEN output contains the nuclide inventory of > 1000 nuclides of each batch. In case of an HTR-Module calculation model, where each fuel channel is subdivided into 20 regions, the inventory curve (in green), is determined by 20 data points. STACY uses the calculated inventory at the start and end of each interval to calibrate the inventory of a sphere within the fission product release calculation to results determined by the depletion code.

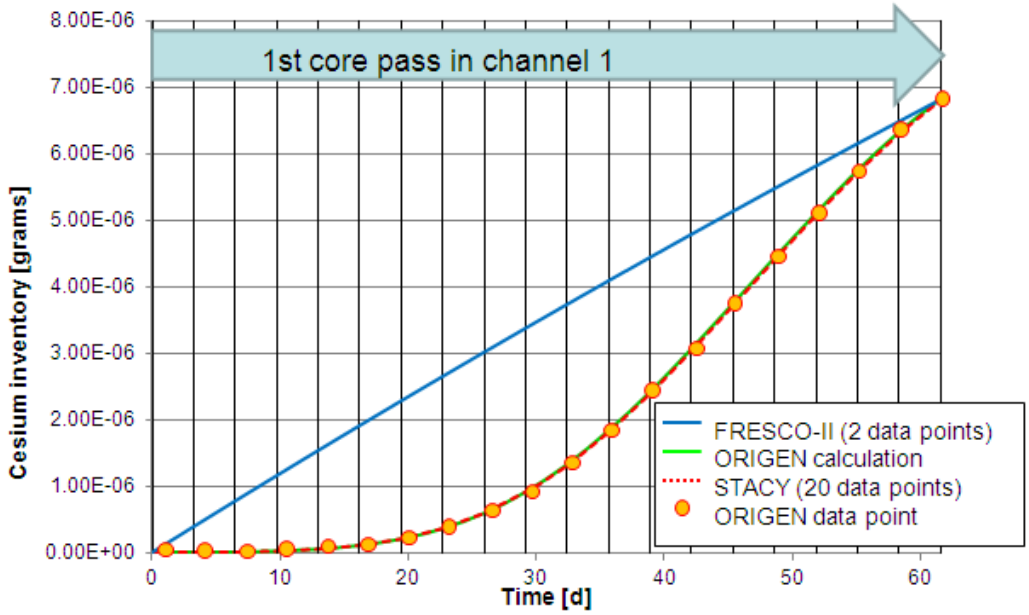

Fig. 17: Cesium 137 inventory as a function of time (HTR-Module fuel element) [15]

STACY performs many simulation steps during one fuel shuffling step (residence step of a fuel element in one region) and “interpolates” the inventory according to the equation above. The resulting curve is displayed in red. Although the extended approach is rudimentary, the curve follows the calculated inventory curve seamlessly because the curve is adjusted each interval. The imaginary source term, which is one of the main values which determine the fission product release calculation, delivers a fission product concentration profile, whose integrated value is equal to the nuclide inventory defined by the burnup code. Due to the very low release rates, there is no need to take the release rate into account for the burnup calculation.

Especially for short-lived nuclides, like for example I-131, the discrepancy between the inventory calculated after the simplified equation and the inventory calculated by using a depletion code can be large in case of a MEDUL (“Mehrfachdurchlauf” = multiple pass) reactor, see Fig. 18 [15]. While calculating the FP release of one sphere with FRESCO-II, only one single inventory was provided to the code, which was most of the time the inventory at the end of the irradiation phase. Internally, FRESCO-II does determine the inventories for all time steps in between. Fig. 18 (blue curve) shows the result in case the time-averaged inventory is provided to FRESCO-II. To the short half-life of I-131, the inventory provided via the input is achieved very early and is constant from that time. The red curve is showing the correct inventories.

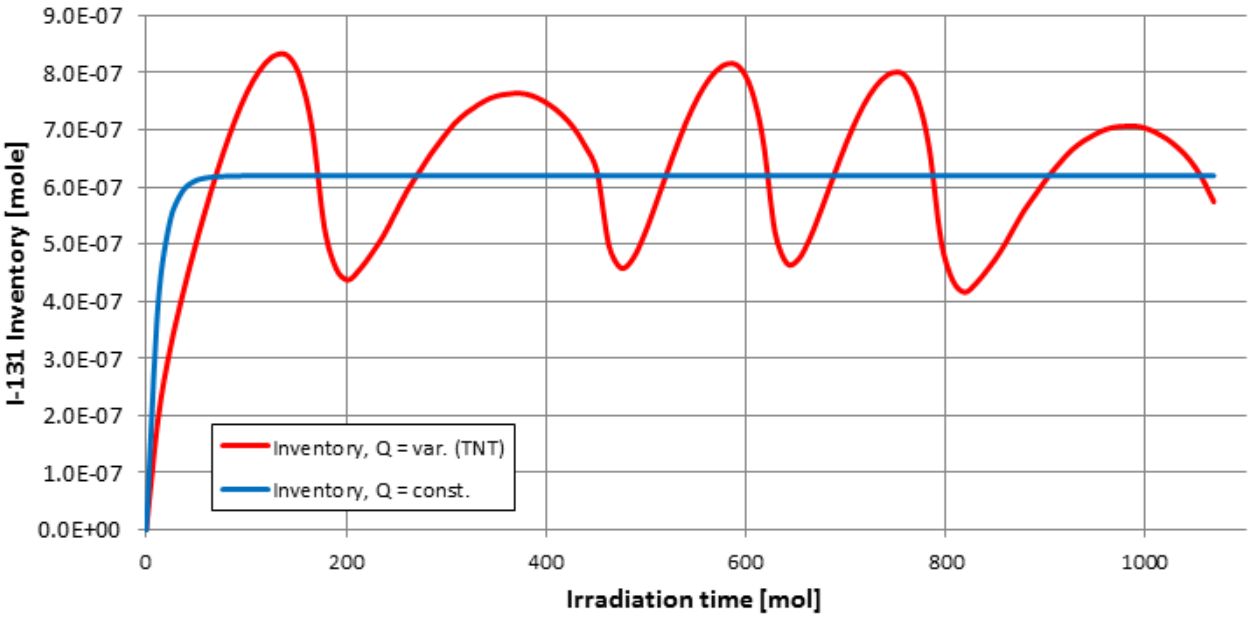

Fig. 18: Iodine 131 inventory as a function of time (HTR-10 fuel element)

According to the burnup calculation the inventory is lower than formerly assumed at the position where the fuel temperature is highest (in case of a reactor core where the coolant flow is downwards). This results in lower I-131 release rates.

Especially in case of a running-in phase, a correct description of the time-depending nuclide inventories is necessary. An analytical equation cannot describe the time-depending inventories during a running-in phase with varying power levels and shutdown phases at all.

4.1.2 Fuel shuffling model

In both the VSOP and STACY model, the fuel movement is modelled after the so-called stream tube model. In case of VSOP, the pebble bed is divided in fuel channels, in which the fuel moves at a constant velocity. The continuous flow of the fuel is modelled by moving the fuel step-wise from one region to the one below. Due to the fact that data like neutron fluxes are used from VSOP, the fuel management being used in STACY is also based on the stream tube model. First of all, the fuel shuffling approach used in VSOP will be explained.

In VSOP, the core is divided into several “imaginary” fuel channels. The flow velocity within each fuel channel is uniform. Each of these channels is subdivided in so called regions (spectral zone). The continuous pebble flow is modelled by a discontinuous shuffling of the content of the regions. A region can hold one or several batches (burnup zone), to represent dummy elements, different fuel types and fuel elements at different burnup levels. The batches within a region a treated as a homogenous mixture, this means that a batch has no distinct position within a region. Each batch has its individual nuclide vector for which an individual burnup calculation is performed. The batches are shuffled according to a user-defined fuel shuffling scheme.

Fig. 19 shows the burnup as a function of the core pass number for the first two core passes in case of the HTR-10 equilibrium core. Due to the mixing, the burnup of the fuel at the beginning of each core pass is equal for all fuel channels. The mixing results in a small variation of the burnup after 5 core passes (nominal value). At the end of the 5th core pass, the burnup is equal to 76,917 MWd/t_{HM} in channel 1 and 80,796 MWd/t_{HM} in channel 5. The maximum burnup is achieved in the outermost channel, because of the residence time, which is a factor of three higher than the residence time of the fuel elements within the innermost channel. In case of a taller HTR, like the HTR-Module, the residence times are comparable for the different fuel channels. Due to the higher neutron fluxes in the centre of the core, the burnup levels achieved in the innermost channel are higher than the ones achieved in the outer fuel channels, if the residence times are comparable.

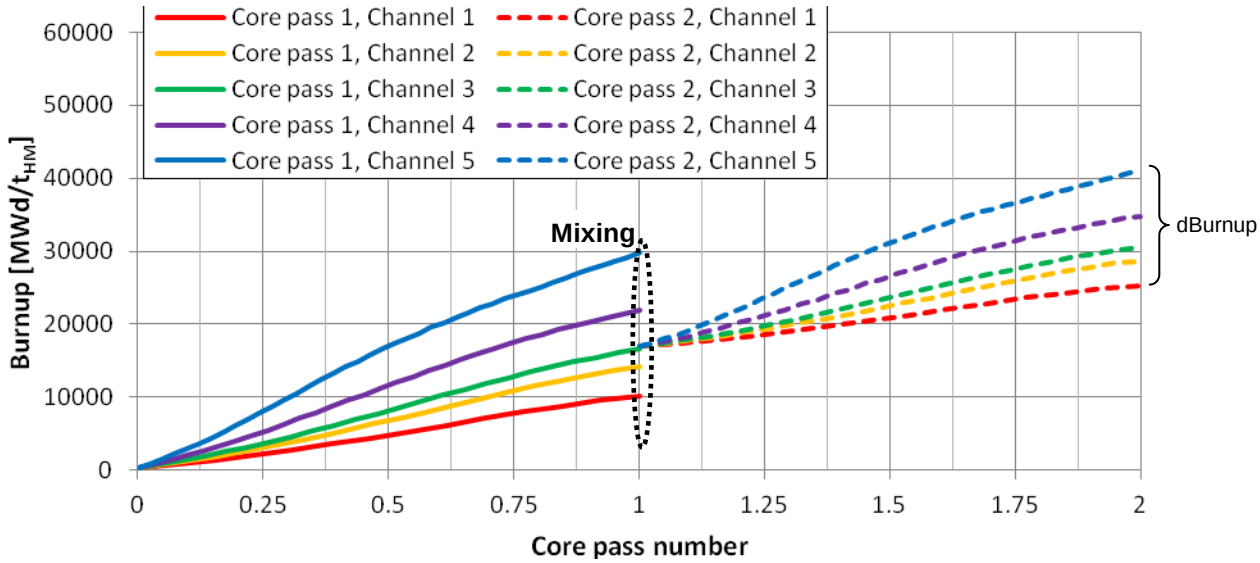

Fig. 19: Burnup as a function of the core pass number for the first two core passes
(batches with mixing of batches at the end of each core pass, HTR-10 equilibrium core)

In comparison to this, the burnup for individual pebbles looks different. Fig. 20 displays the burn up as a function of the core pass number for fuel which is not mixed at the end of each core pass. For the first core pass, only the curves for fuel in channels 1 and 5 are displayed and for the second core pass all possibilities are displayed. It can be seen, that the variation in burnup is higher by using this approach.

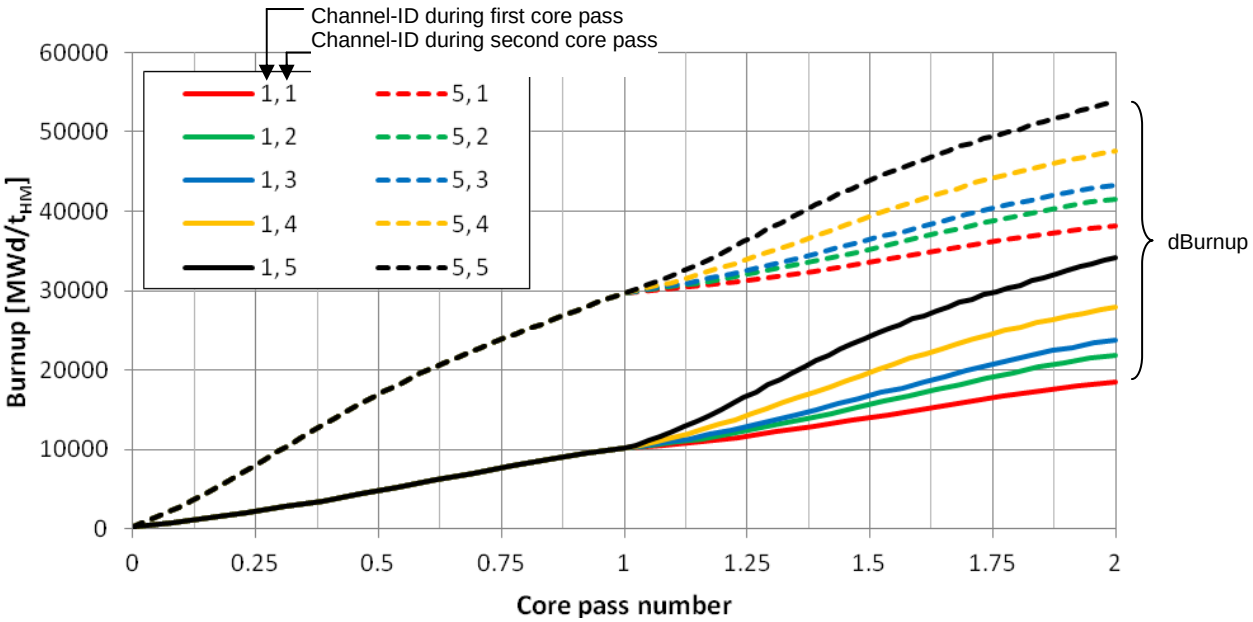

Fig. 20: Burnup as a function of the core pass number for the first two core passes (individual fuel elements without mixing at the end of each core pass, HTR-10 equilibrium core). For the first core pass, only channels 1 and 5 are displayed and for the second core pass all possibilities are displayed)

Adopting this approach for the simulation would lead to a fast increasing number of fuel batches with an increasing number of core passes. Eventually, the code would treat each fuel element separately. From the simulation point of view, e.g. a burnup calculation has to be performed for each batch and time step which is time consuming and cannot be handled. Normally, the properties of the batches are mixed at the end of each core pass in case of an HTR with MEDUL fuel strategy. Batches of all fuel channels which get unloaded at the lower end of the core are mixed and average batches are determined. Due to the mixing, properties like the nuclide vector and burnup are homogenized, which leads to a loss of information.

In case of a particle failure fraction or fission product release calculation it is not trivial to determine an average batch (representative fuel element) which behaves like the sum of the batches which are part of the mixture. It would be necessary to mix properties like the fission product concentration profile along the fuel element radius and the number of failed coated particles. In addition, it is necessary to take multiple fuel element histories into account to achieve best-estimate values for fission product release rates. Rather exceptional cases are taken into account, which can influence the overall fission product release perceivably. Due to the statistical mixing of batches after each core pass in the VSOP-calculation it is not possible to simulate the fission product release of one specific batch.

As mentioned before, the fuel management in STACY is modelled after the same stream tube model. Nevertheless, there are some differences between the two models, which will be explained in more detail. The approach chosen for STACY differs from the VSOP-approach regarding the way fuel is discretized (see Fig. 21).

The fuel is represented by so-called tracer pebbles, which have a distinct position within the core. These pebbles are shuffled through the core along flow lines. These curves correspond to the limiting curves of the flow channels. By interpolation, intermediate flow curves are calculated in between the user-defined flow curves. The tracer pebbles are not mixed with other pebbles at the end of each core pass. Instead the burnup is checked and compared with the burnup target. If the target has not been reached, the pebble is reintroduced into the core. The new radial position of the tracer element is being determined by a random number generator.

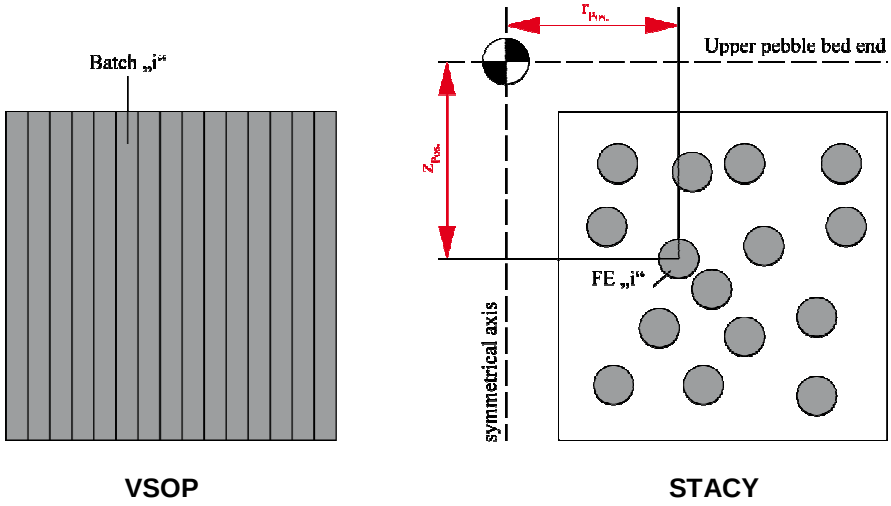

Fig. 21: Comparison of fuel representation in a region between VSOP and STACY [15]

Nevertheless, macroscopic values generated by VSOP are valid. Each single tracer fuel element on its own will not change the overall core behaviour. Thus a returning of data to VSOP is redundant. In principle, this procedure has been used for years by performing fission product release calculations, but only for a limited number of fuel elements which were user-defined. To perform coated particle failure fraction and fission product release calculations, input files were prepared for each individual fuel element by using fuel temperatures being calculated by codes such as VSOP or THERMIX. The user defines one or several representative fuel elements which are able to represent the fission product release behaviour of all fuel. Most of the time, stringent boundary conditions were chosen, such as assuming that the pebble goes only along the flow curve with the highest fuel temperatures. This approach results normally in an upper limit for the release rates.

The main routines of STACY, although completely being rewritten in FORTRAN 2003, is based on the same physical phenomena as modelled in FRESCO-II [15]. Both the release of Fickean diffusion and recoil are taken into account. The diffusion coefficients of the radionuclides for the different coated particle layers and the matrix material of the spheres are being modelled in form of Arrhenius equations. Coated particle (CP) failure fractions can be determined according to the PANAMA approach, which uses to be a stand-alone code and has become now an integral part of the STACY code. As another option, coated particle failure fractions can be provided as a burnup (or time)-dependent curve or can be determined by applying the so-called “Trumpet Curve”, a burnup and accident temperature-dependent function, as was defined by Interatom.

After the modernization and merging of FRESCO-II and PANAMA to one single program (STACY), routines have been implemented which read the necessary data from a VSOP-output. STACY is able to perform calculations for a vast number of single tracer fuel elements automatically. Due to the fact that a large number of tracer fuel elements are taken into account, the code considers spatial distributions for fuel temperatures and nuclide inventories within the core.

4.1.3 Adaptation made to simulate running-in phases

The simulation of the running-in phase poses some additional challenges in comparison to the simulation of the equilibrium core. Even if adaptations and extensions made to codes are not part of the ARCHER framework itself, there is a need to describe the improvements and extensions made to this code system to gain a better understanding of the model being used in this study.

As a new feature of STACY, it is possible to calculate the fission product release during the running-in phase of an HTR core, including varying power levels, pebble shuffling rates and shut down phases. In addition, dummy elements can be considered. These features enable to calculate the fission product release during the operating history of the HTR-10 and to describe the current state of the fuel within the reactor.

STACY is being coupled via reading both the input and output file of the multi-physics code VSOP [3]. This code is mainly being used for reactor design and to simulate the behaviour of the core under normal operating conditions. It is also possible to simulate some accident scenarios where neutronics do not play a

role and do not need to be considered, like for example DLOFC (depressurized loss of forced cooling) accidents. For the calculation of the fission product release rate for the equilibrium core, it is sufficient to transfer solely one set of spatial broad group fluxes, fluid temperatures and so on.

Due to the fact that these spatial distributions vary over time during a running-in phase, these data sets have to be calculated for each individual time step by VSOP. To handle this larger amount of data, the data structure behind STACY has been reorganized. For each shuffling time step, an individual data object is initialized and filled with data read from the VSOP output file. Due to the amount of data to be transferred between VSOP and STACY in case of the running-in phase, routines have been implemented which can extract the data automatically from the VSOP output file.

One of the main differences between the two codes is that STACY shuffles individual tracer pebbles instead of batches. In case of an equilibrium core, the instructions which define from where to what position is being moved have only to be defined once and are per definition constant over time. Due to the complexity and irregularity of the fuel shuffling scheme of the HTR-10, it is necessary to read all these individual sets of instructions and to be able to process them. The irregularities pose some exigencies to the STACY model, which will be explained later in more detail.

The tracer pebbles are loaded in a similar way as the batches. The user-defined number of tracer pebbles is divided over the different batches according to the initial batch loading scheme. Due to the fact that natural numbers are used and rounding effects, it can occur that the user-defined number is not met exactly. After having divided the total number of tracer pebbles over the different batches it is checked whether the sum all individual tracer pebble numbers coincides with the user-defined number. If needed, the individual tracer pebble numbers are adapted. Next, the tracer pebbles are loaded to the core. Each tracer pebble is linked to a batch-ID which allows using the fuel shuffling instructions as they are defined within the VSOP input file for the batches.

The tracer pebbles are moved almost continuously (see Fig. 22). The time step width used for the fission product release calculation is smaller than the residence time of a tracer pebble in a region. It is assumed that the tracer pebbles which are located at an equal vertical position before a fuel shuffling step are located at another, but equal position after the fuel shuffling step (see Fig. 22).

During this fuel shuffling step, the tracer pebbles move over a certain vertical dz_1. Due to reasons of volume conservation and the tapering of the fuel channels, the vertical distance over which tracer pebbles are moved during a fuel shuffling step increases during a core pass as long as other parameters such as $\Delta t_{Shuffling}$ and $\Delta t_{Res,Region}$ remain unchanged.

The flux distributions being determined by VSOP are being used to calculate a time depending nuclide vector for each individual tracer pebble by using the newly developed depletion code Topological Nuclide Transmutation (TNT) [14]. The irradiation history of the sphere is stored as a vector of broad group fluxes. At the following event, another set of broad group fluxes is added to the vector:

1) At the beginning of a new interval during the operational history
2) At the beginning of a new core pass
3) As soon as the lower boundary of a region is crossed, the broad group fluxes of the region below are added.

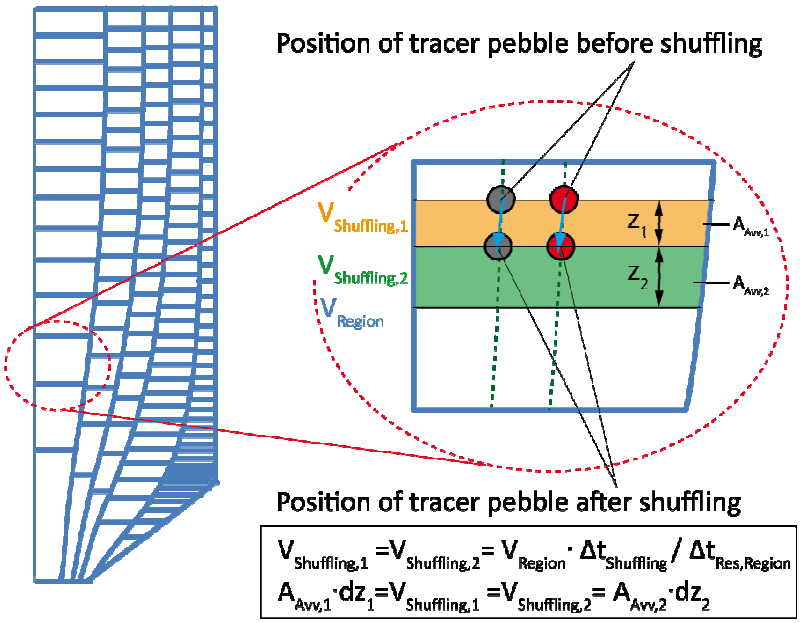

Fig. 22: Semi-continuous fuel shuffling in STACY

The initial nuclide vector of a fresh HTR-10 fuel element which has been used for the depletion calculations is displayed in Table 6.

Table 6: Initial nuclide vector of HTR-10 fuel element being used for depletion calculation with TNT

Nuclide	Inventory [mole]
U-234	3.65368E-05
U-235	3.61526E-03
U-238	1.73916E-02
Silicon	4.59633E-02
Boron	8.52778E-06
Carbon	1.61491E+01
Oxygen 16	4.20869E-02

In addition, it is necessary to switch to the newly implemented xml-input format of the burn up code TNT. The ASCII input format which was part of the first version of the TNT code did only allow for a constant time step width, which is sufficient in case of an equilibrium core. The varying fuel shuffling rates of the pebble bed, however, require the usage of the new TNT input format.

So far, STACY could not take the presence of dummy elements into account. To study the HTR-10 starting from initial criticality, dummy elements which are part of the initial core should be taken into account. The fraction of dummy elements is lowered during the operation time of HTR-10. As a new feature, it is possible to treat both fuel and dummy elements within one model. Nevertheless, it is not possible to treat different fuel element types.

As a new part of STACY, the so-called transformation matrices which enable to map data from one grid to another can be determined by the code itself base on the same data. For example one matrix is being generated which enables to transform data between the regions and the fine Cartesian meshes of the active core.

4.2 Fission product release calculations of HTR-10

In this section, fission product release results are presented. First of all, an overview of input parameters which are equal for both the equilibrium core calculation and the running-in phase will be presented. Next, fission product release rates have been calculated for the equilibrium core as a first step. Finally, fission product release rates during the running-in phase will be presented.

4.2.1 Description of main input values

4.2.1.1 Particle failure fraction

A main parameter within the fission product release calculation is the particle failure fraction distribution, due to the high retention level of intact coated particles. In STACY the coated particle failure fraction can be calculated after the PANAMA-model or the so-called Trumpet Curve. The trumpet curve has been derived by Interatom for the HTR-Module and models the failure fraction as function of the fuel temperature and the burnup level (see Fig. 23a). The curve does not take into account, how long the fuel is exposed to certain temperatures. As soon as a certain temperature has been passed the corresponding failure fraction is assumed.

For the HTR-10 under normal operating conditions, the fuel temperatures stay well below 1200°C. For these fuel temperatures, the particle failure fraction is only depending on the burnup level. The trumpet curve assumes that the failure fraction is increasing linearly with the burnup level. These failure fractions do correspond with the values in Table 9. For this reason, the trumpet curve has been modified to fit with INET specifications (see Fig. 23b). A fresh fuel element has a coated particle defect fraction of 3.0×10^{-4} and a spent fuel element has a defect fraction of 8.0×10^{-4}.

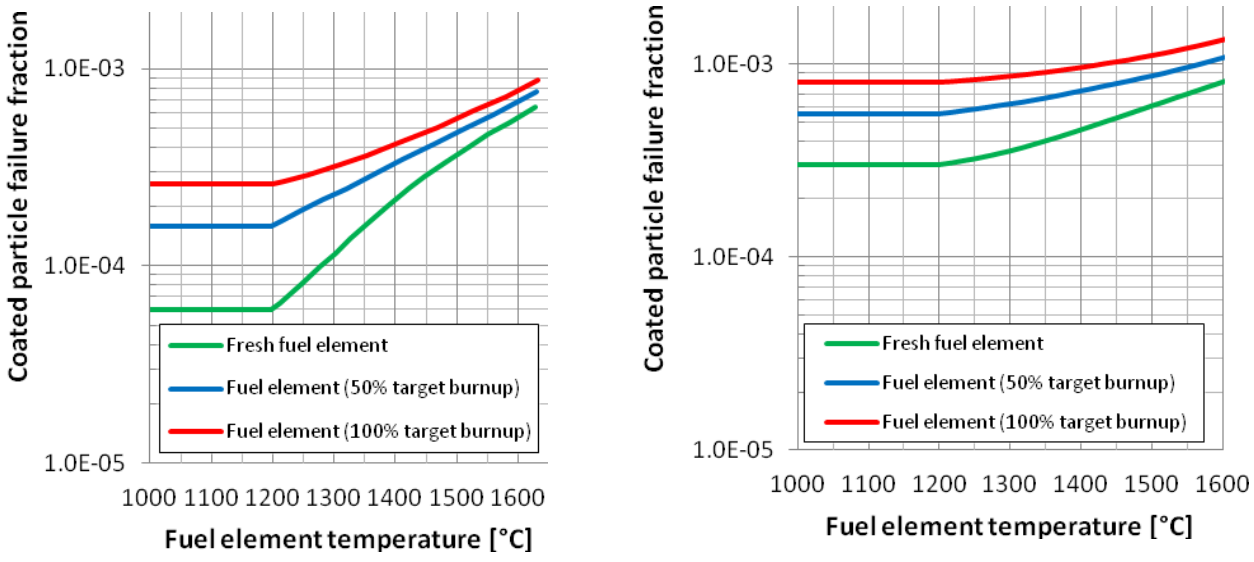

a) HTR-Module [8] b) HTR-10 (deduced from HTR-Module)

Fig. 23: So-called “Trumpet Curve” describing the coated particle failure fraction as a function of the fuel temperature and the burnup level

In comparison to FRESCO-II, the number of batches with defective particles treated in the fission product release calculation is no longer limited to a fixed number but can be adapted by the user. Nevertheless, for each batch of defective particles (particles which got damaged during the same time step) a representative particle is simulated. To limit simulation time on one hand without losing accuracy on the other hand, the user has to define an acceptable number of thresholds. After passing a threshold, an additional batch with defective particles is being treated in the diffusion calculation. Fig. 24 shows an example of thresholds superimposed to the trumpet curve as it has been derived for the HTR-10. The number of defect coated particle batches is thus limited by the number of thresholds. The actual coated particle failure fraction is determined by linear interpolation of the trumpet curve. If the actual fraction of defect particles exceeds the average between the value of defects particle of the current and next threshold, the value of the next

threshold is taken instead of the calculated number of defect particles. From this time point, an additional batch of defective particles is considered in the fission product release calculation.

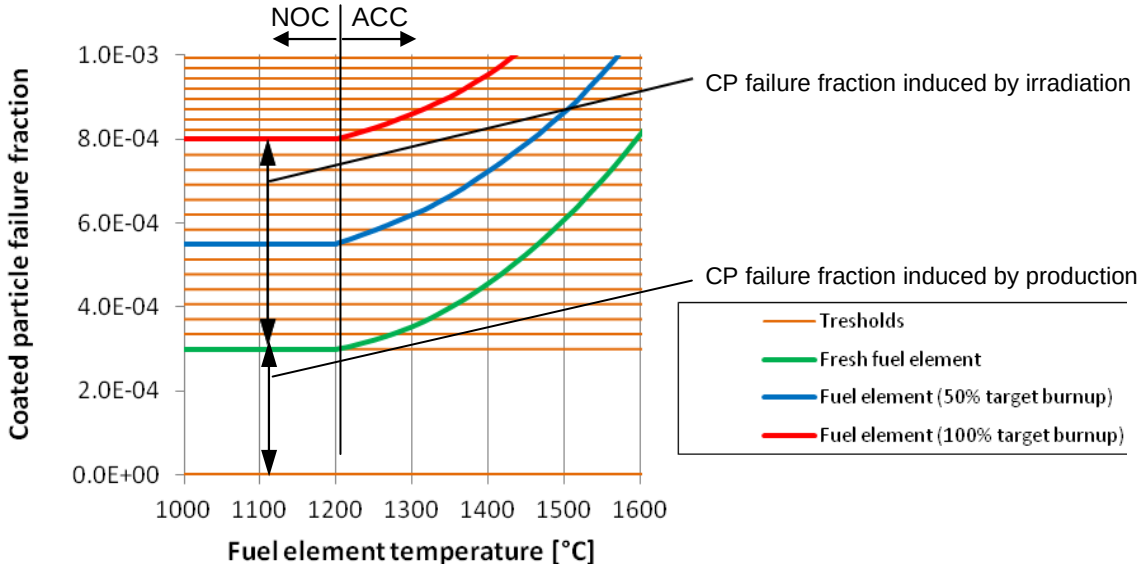

Fig. 24: Thresholds for coated particle failure fractions in the fission product release calculation superimposed to the trumpet curve of HTR-10

4.2.1.2 Determining the disadvantage factor

Due to the fact that no spectral code is currently coupled to either the STACY or TNT code, a disadvantage factor, which takes the double heterogeneous structure and thus the self-shielding of the fuel elements into account, has to be determined. Only one constant disadvantage factor is taken into account, which is used for all fuel elements. By doing so, the energy dependency of this factor is neglected. All neutron induced reactions within TNT are multiplied with this factor, which affects the burnup and nuclide inventory history.

The disadvantage factor has been derived by the following procedure. For several sets of 500 tracer fuel elements with an individual life history, TNT calculations are performed. The resulting burnup levels after 5 core passes (average core pass number) have been ordered from the lowest burnup to the highest burn up for each set (see Fig. 25). A disadvantage factor of 0.65 resulted in an average burnup of 7.58 % FIMA, which is too low. Neglecting the self-shielding (disadvantage factor = 1.00) resulted an overestimation of the burnup of the tracer fuel elements (10.81 % FIMA). As a final value, a disadvantage factor of 0.78 has been conducted which meets the burnup target of 8.9 % FIMA.

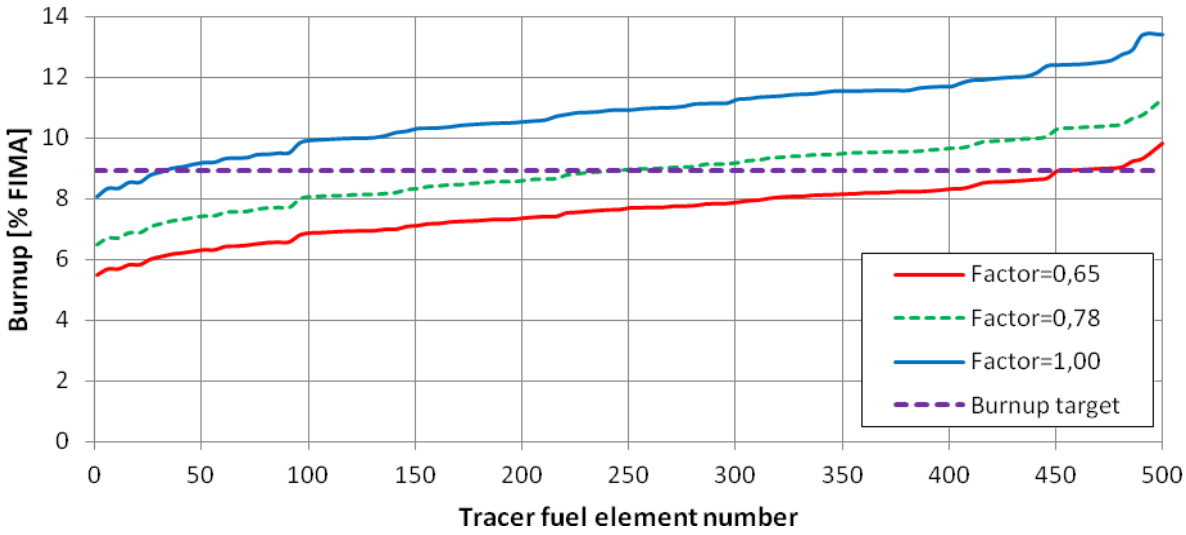

Fig. 25: Burn up distribution of 500 tracer fuel elements for three different disadvantage factors (tracer fuel elements are sorted after burn up)

4.2.1.3 Diffusion coefficients

In STACY, the fission product release is based on Fickean diffusion and recoil. For this Fickean diffusion calculation, diffusion coefficients, which are an essential part of the fission product release calculation, have been taken from IAEA TECDOC-978 [16]. These so-called “effective” diffusion coefficients were deduced from results from, e.g., heating experiments with spherical fuel elements and coated particles. “Effective” means that all possible transport mechanisms are summarized in a simplified single transport process [16]. Diffusion coefficients depend mainly on the fuel element design and production methods. Thus, a slight adaptation of these parameters can affect the fission product retention capability. For this reason, diffusion coefficient cannot be transferred to other fuel design etc. per definition. Each time, the quality of the fuel by means of fission product retention has to be demonstrated. For this reason, the irradiation of Chinese fuel elements has been conducted in the HFR in Petten lately. These spheres will undergo heating tests to demonstrate the fission product retention capability of Chinese HTGR fuel. Within this report, it is assumed that the retention of Chinese fuel is comparable to German fuel and that the diffusion coefficients being published in [16] can be applied for the HTR-10 fuel elements (see Table 7) as well. In the case that no value is being specified, it is assumed that the retention is nearly perfect. The diffusion coefficients are described by an Arrhenius equation:

$$D(T,\Gamma) = \sum_i D_{0,i}(T,\Gamma) \cdot e^{-\frac{Q}{R \cdot T}}$$

with

D_0	frequency factor (pre-exponential factor)	[m^2/s]
T	temperature	[K]
Q	activation energy	[J/mol]
R	gas constant	[J/(mol·K)]
Γ	fast neutron fluence (E > 0.1 MeV)	[10^{25} m^2]

The diffusion coefficients in [16] comprise one (i = 1) branch, describing the complete temperature range of interest or two (i = 2) branches / regimes, where an individual branch is defined for both low and high temperatures. In case of cesium, a slight dependency of the diffusion coefficient of the fast neutron fluence is taken into account (see Table 7).

Table 7: Diffusion coefficients [16], Γ : fast neutron fluence

	Cesium		Strontium		Iodine		Silver	
	D_0 [m^2/s]	Q [kJ/mol]	D_0 [m^2/s]	Q [kJ/mol]	D_0 [m^2/s]	Q [kJ/mol]	D_0 [m^2/s]	Q [kJ/mol]
UO_2	5.6×10^{-8} 5.2×10^{-4}	209 362	2.2×10^{-3}	488	8.8×10^{-15} 6.0×10^{-1}	54 480	6.7×10^{-9}	165
LTI PyC	6.3×10^{-8}	222	2.3×10^{-6}	197	-	-	5.3×10^{-9}	154
SiC	$5.5\times10^{-14}\cdot e^{\Gamma/5}$ 1.6×10^{-2}	125 514	1.2×10^{-9} 1.8×10^{6}	205 791	-	-	3.6×10^{-9}	215

4.2.1.4 Description of INET calculation and input values used

No publications could be found regarding fission product release during the running-in phase. A paper has been published with respect to the fission product release of the equilibrium core [12]. Within the studies being performed as a part of that publication, the tool FRESCO-II has been used to predict fission product release rates. First a short overview of INET input data is provided.

As a first step, the fission product release rate of selected nuclides is being calculated for the equilibrium core. Fission product release rates are being calculated by INET using FRESCO-II, STACY predecessor. The maximum central fuel temperature is equal to 864°C according to INET simulations. The temperature distribution determined is shown in Table 8. For reasons of conservatism, this distribution has been replaced with a distribution where the temperature exceeds the upper temperature of the former temperature range, and the fractions are rounded in such way that a larger fraction is facing a higher temperature.

Table 8: Fuel temperature distribution from fluid dynamical calculation being used for fission product release calculation [12]

Temperature range	Fraction of the fuel (calculated)	Temperature	Fraction of the fuel (used in FP rel. calc.)
815.5°C < T < 864.0°C	0.1 %		
758.6°C < T < 815.5°C	5.9 %	820°C	7.0 %
644.9°C < T < 758.6°C	29.4 %	760°C	30.0 %
T < 644.9°C	63.7 %	700°C	63.0 %

For the fission product release calculation, coated particle failure fractions as shown in Table 9 are used.

Table 9: Coated particle failure fraction used in INET calculations [12]

Free uranium (as manufactured)	3.0×10^{-4}
Failure fraction due to irradiation	5.0×10^{-4}
Failure fraction (end of life (EOL))	8.0×10^{-4}

Within the paper, absolute fission product release values are presented. For this purpose, the core inventory has been determined by an ORIGEN-2 calculation for a fuel element which goes only through the third fuel channel.

4.2.2 FZJ calculations

4.2.2.1 Equilibrium core

The previous section 4.2.1 provided an overview of data which is used for both the equilibrium core calculation and the simulation of the running-in phase. First of all, some parameters which depend on the operating conditions, such as the fuel element temperature distribution, which influence the fission product retention, will be discussed in this section. After this, results are shown for one randomly selected tracer fuel elements and eventually, fission product release from the complete core will be discussed and compared to values that were published by INET.

Fuel element temperatures

One of the main parameters is the fuel element temperature. The central temperature is decreasing slightly with increasing burn up (see Fig. 26). In general, a VSOP batch contains fuel or dummy elements of the same type with the same time history. The equilibrium core of the HTR-10 does not contain dummy elements and contains only fuel element of one type. In this case, a batch number is directly related to the number of core pass achieved.

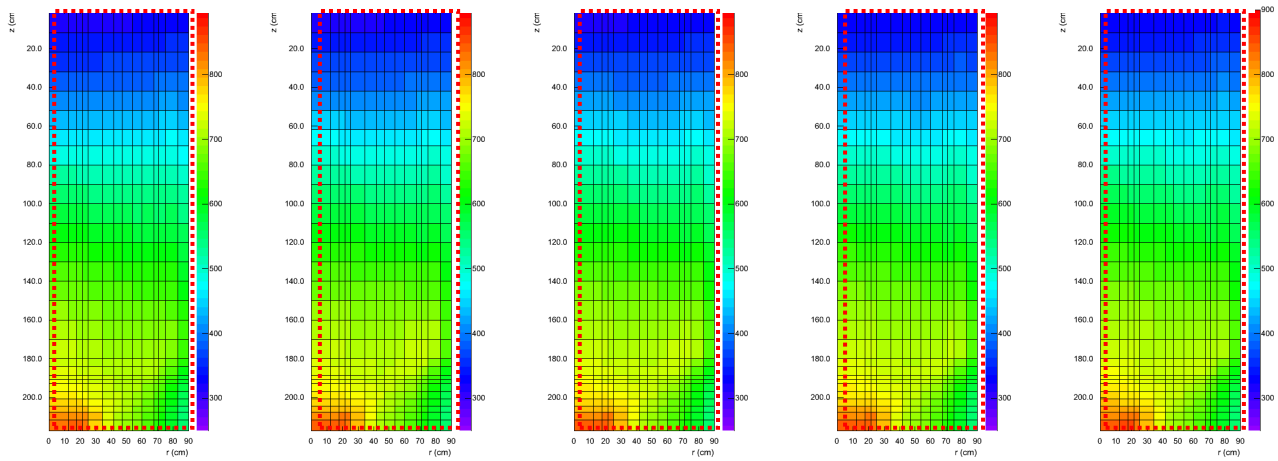

Batch 1 **Batch 2** **Batch 3** **Batch 4** **Batch 5**

Fig. 26: Central fuel element temperatures for 5 different batches / core passes (HTR-10). Values have been simulated by VSOP (core is not drawn to scale)

Fig. 27 confirms that the fuel element temperatures for different core passes do not differ much. In comparison to this, fuel elements temperatures are very different in case of the HTR-Module. The time-averaged power of a single HTR-Module fuel element is about double the value of an HTR-10 fuel element.

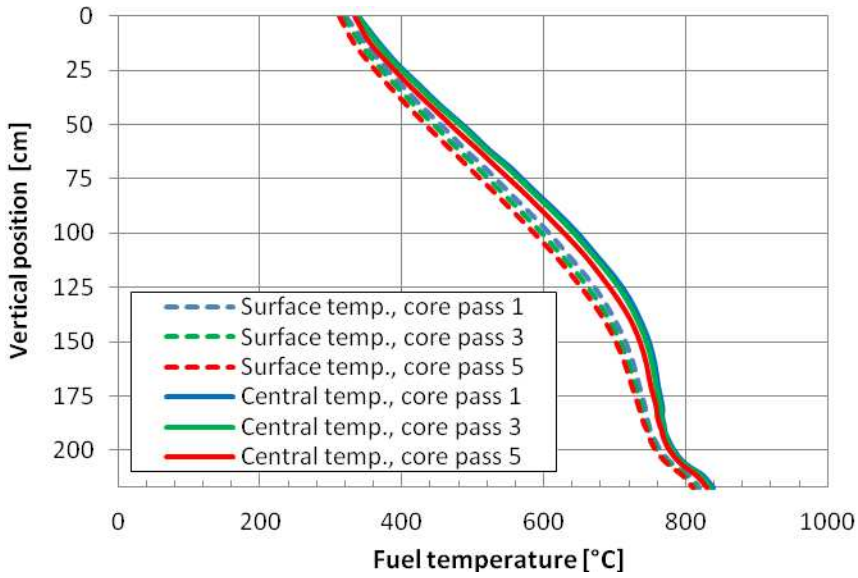

Fig. 27: Surface and central fuel element temperatures along the symmetrical core axis for fuel elements with a different core pass number

Neutron flux

For the depletion calculation, broad group fluxes are used. The time depending broad group neutron fluxes are generated by shuffling the tracer fuel element through the core, where the spatial broad group neutron flux distributions are per definition constant over time in case of the equilibrium core. These distributions have been determined by VSOP (CITATION) for the equilibrium core (see fig. Fig. 28).

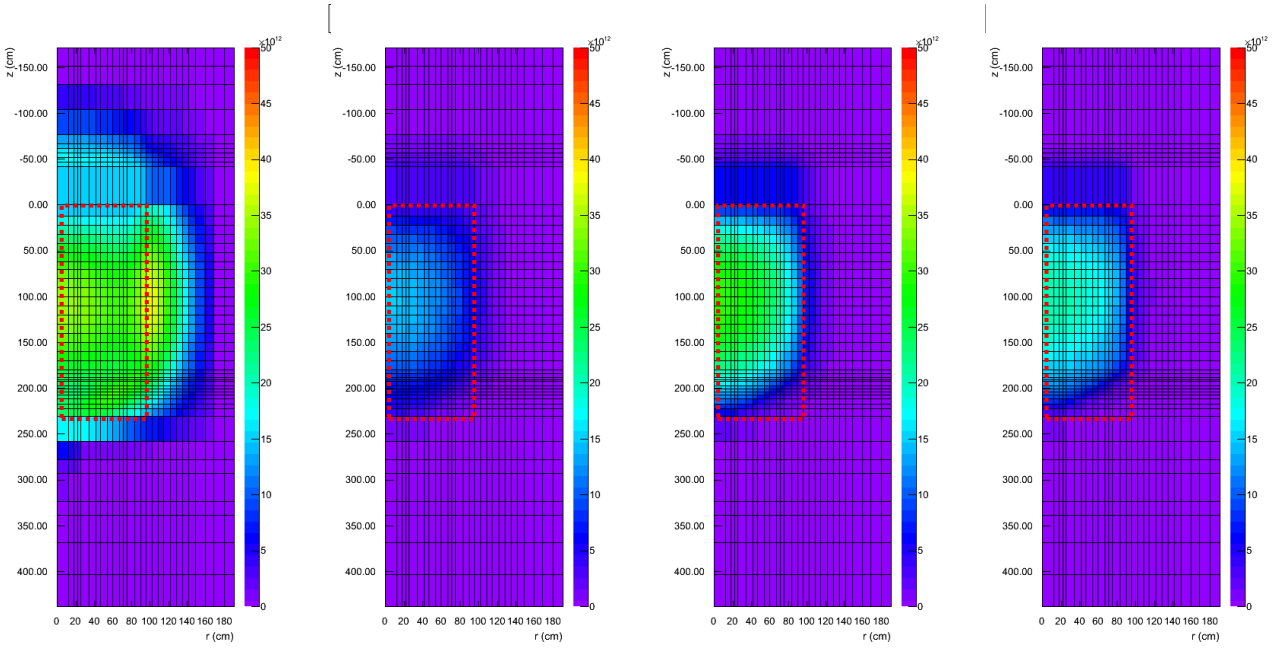

Thermal flux ($2.5x10^{-3}$ eV < E ≤ 1.9 eV)

Epithermal flux 1 (1.9 eV < E ≤ $1.30073x10^{2}$ eV)

Epithermal flux 2 ($1.30073x10^{2}$ eV < E ≤ $2.35177x10^{5}$ MeV)

Fast flux ($2.35177x10^{5}$ MeV < E ≤ $1.0Ex10^{7}$ MeV)

Fig. 28: Spatial broad group neutron flux distributions within the HTR-10 equilibrium core

The picture shows the different broad group neutron fluxes for a random fuel element of the HTR-10. This fuel element goes through fuel channels 2, 4, 5, 1 and 3. It can be seen, that the residence time in fuel channel 1 is shortest and longest in channel 5.

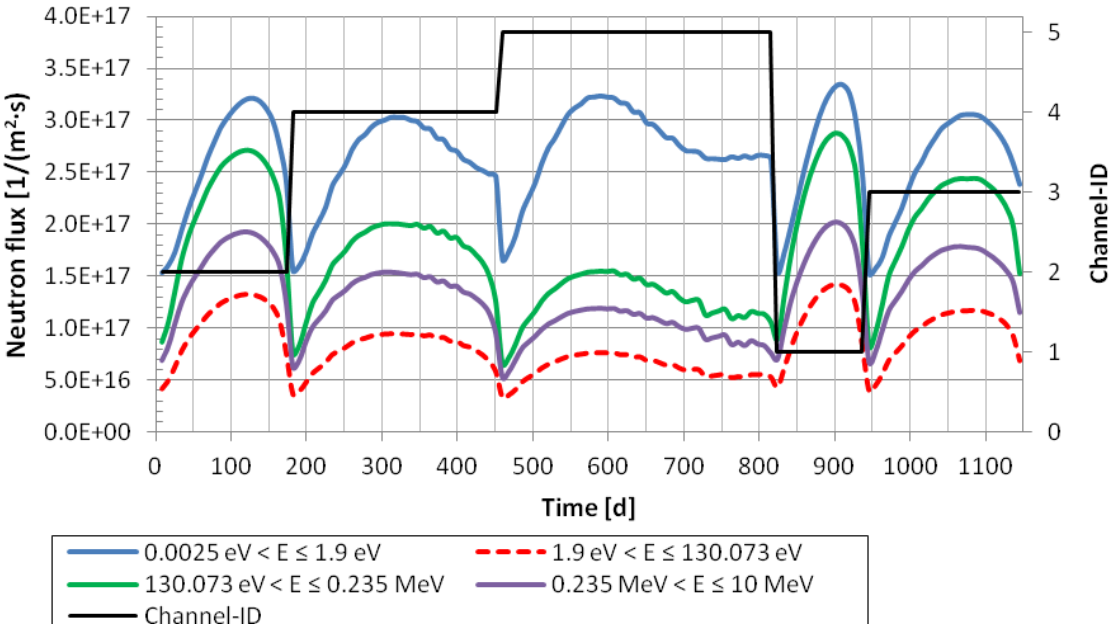

Fig. 29: Broad group neutron fluxes for a randomly chosen fuel element of the HTR-10

The resulting nuclide inventories are being displayed in Fig. 30. The inventory of the long-lived nuclides Cs-137 and Sr-90 is increasing steadily, while the inventory of I-131 shows some fluctuations.

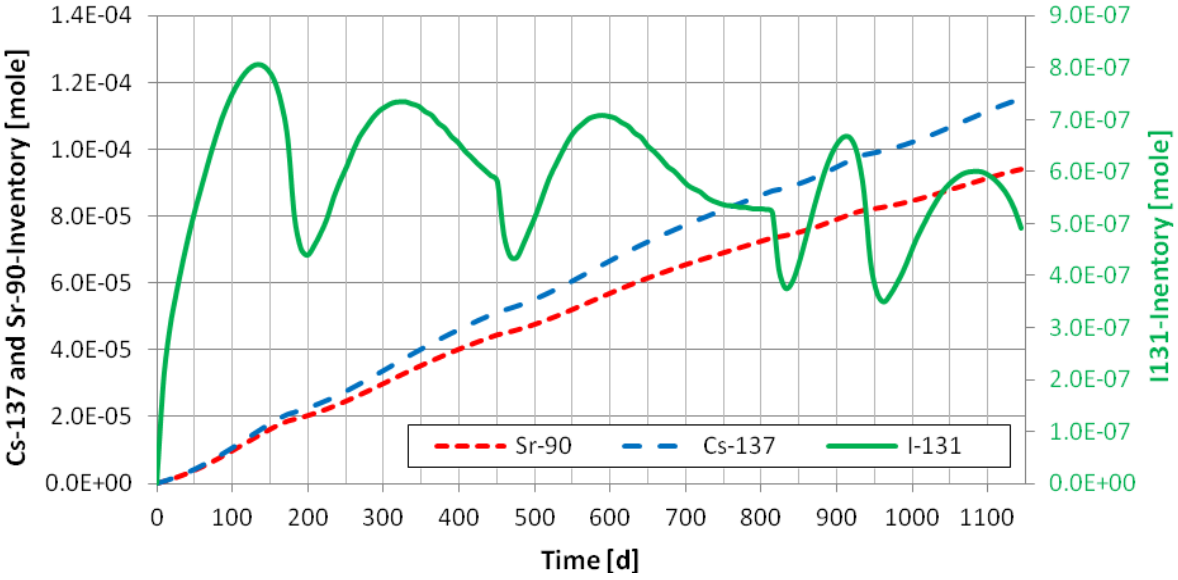

Fig. 30: Nuclides inventories for a randomly chosen fuel element of the HTR-10

The power and burn up level of the same fuel element are shown in Fig. 31. In addition to the time-depending power of this individual sphere, the average power per sphere within the equilibrium core, which is equal to 0.37 kW, is shown.

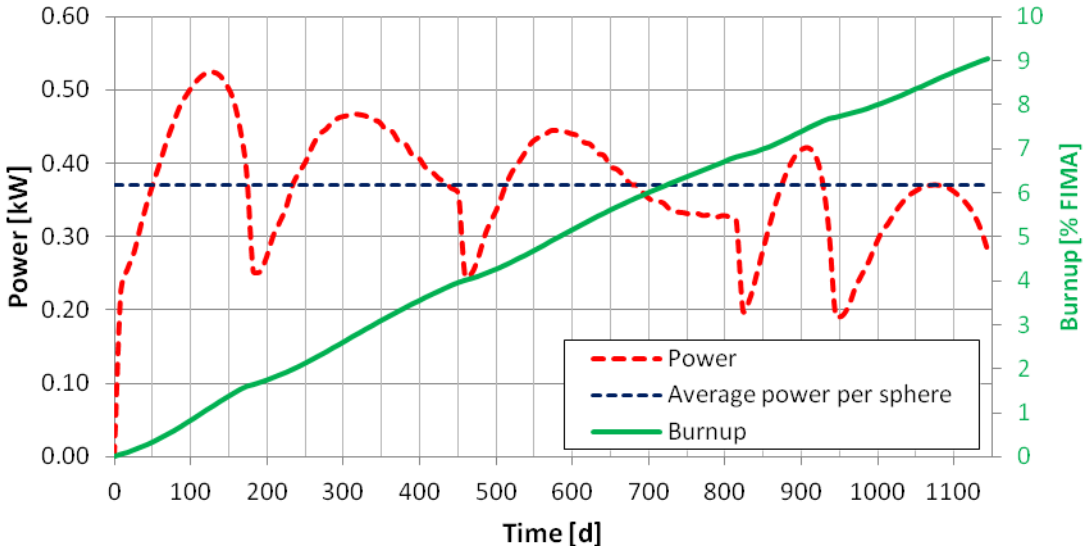

Fig. 31: Power and burn up level for a randomly chosen fuel element of the HTR-10

Fig. 32 shows the Cs-137 release rate during three core passes for a random fuel element. This tracer fuel element flows two times through the second fuel channel and during the third core pass through the fourth fuel channel. The Cs-137 release is maximal at the end of each core pass.

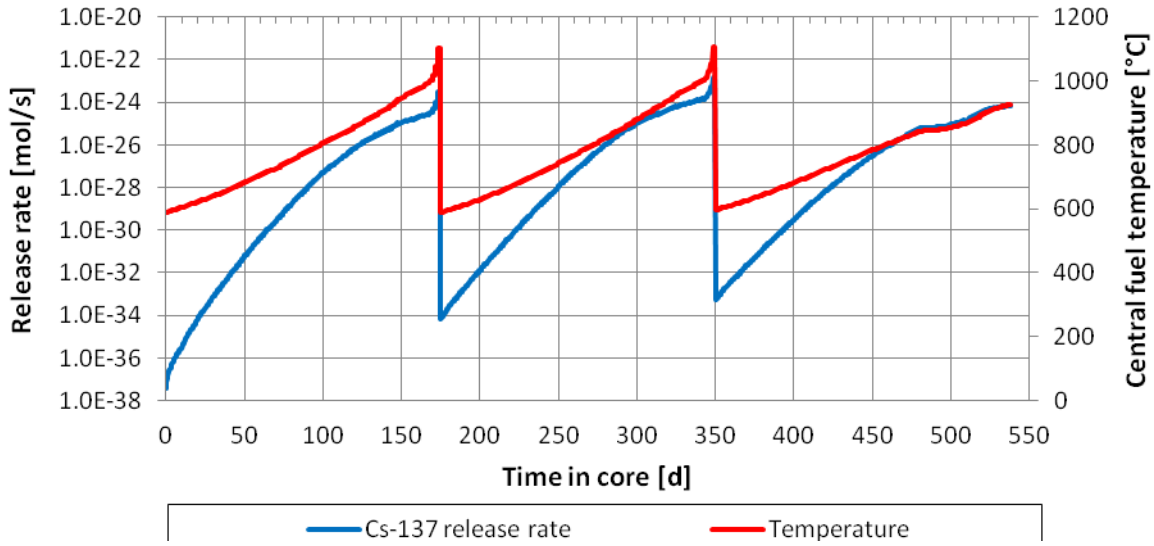

Fig. 32: Cesium 137 release rate and fuel temperature for a random tracer fuel element within the HTR-10 core

Overall results for the core

It is assumed that the conditions are time independent for the equilibrium core. Other effects, which would lead to a time depending fission product release even after the equilibrium core has been reached (plate-off etc.) have been neglected within this study by choosing pure helium as a boundary condition for example.

Combining these results from all tracer elements results in the fission product release rates of the complete core during the running-in phase. A fission product release calculation is only conducted for the fuel elements. The deposition on and diffusion into dummy elements is neglected due to unknown boundary conditions. The dummy elements are shuffled by the fuel management to have a correct representation of the content of each region. This allows for a correct scaling of the fission product release rates from the individual tracer pebbles to overall core release rates.

As mentioned before, in case of an equilibrium core calculation, there are no tracer pebbles in the core at the beginning of the simulation. The tracer pebbles are gradually being introduced to the core at a constant rate. Due to this, the number of tracer pebbles increases steadily until tracer pebbles are discharged, because they have achieved the burnup target. By doing so, the number of tracer pebbles for which a fission product

calculation has to be performed is lower than having a constant number of pebbles within the core from the very beginning. This is only needed to simulate a running-in phase, which will be shown later. In case of a model where each fuel channel has an equal number of regions, equilibrium conditions are attained as soon as the first tracer elements are discharged. At this moment, discharged fuel elements have fulfilled a complete life history and each core zone contains a mixture of fuel elements at a different stage during their life history.

In case of the HTR-10 VSOP and STACY models, where each fuel channel contains a different number of regions, it is more difficult to predict when equilibrium conditions from the fission product release point of view have been attained. Due to the higher residence time, it can be assured that the burnup target is attained after the nominal number of core passes in the outermost fuel channel. Thus, even a fuel element which goes only through the outermost channel has fulfilled a complete life history. Other life histories are shorter.

Table 10 shows a coarse estimation of the maximum time needed to achieve equilibrium conditions. After 1820.7 d, equilibrium conditions are attained per definition. Fig. 33 shows that the fission product release rate is almost constant from a certain time point onwards. This leads to the conclusion that the equilibrium state is reached earlier within the calculation (approximately at 1300 h). This is reasonable because the first tracer pebbles will end their life history much earlier.

Table 10: Estimation of the time needed to establish equilibrium conditions for the fission product release calculation of HTR-10

Number of channels	:	5
Number of regions	:	14 / 20 / 24 / 32 / 42
Maximum number of regions per core pass	:	42
Residence time within one region	:	8.76 days
Nominal core pass number	:	5
Longest life history (outermost channel only)	:	210 regions = 1820.7 days

Fig. 33 shows Cs-137 release rates being calculated for the HTR-10 equilibrium core for different number of tracer pebbles. It can be seen, that results converge by increasing the number of tracer pebbles being used in the STACY simulation. Due to the Monte-Carlo approach being used in STACY smaller fluctuations even occur from the time point where equilibrium conditions have been achieved from the fission product release point of view.

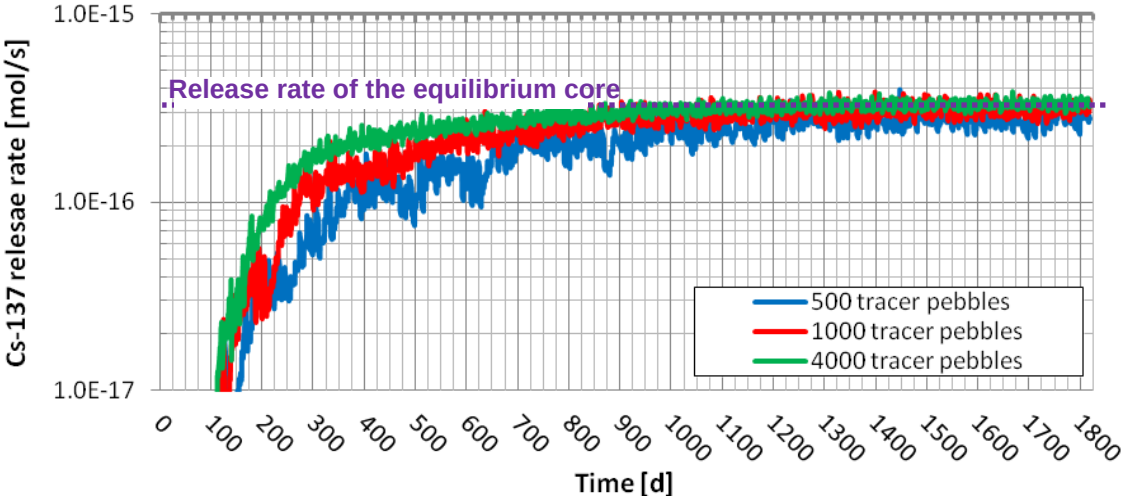

Fig. 33: Cesium-137 release rates for the HTR-10 equilibrium core for different number of tracer pebbles in the core

Fig. 34 shows the distribution of the coated particle failure fractions (Φ). In addition the lower (fresh fuel element, $\Phi = 3x10^{-4}$) and upper boundary values (spent fuel element, $\Phi = 8x10^{-4}$) for the coated particle failure fractions are shown. It can be seen, that the region-averaged coated particle failure fractions fluctuates to some extend, which can be lowered by using a higher number of tracer fuel elements. In case

4000 tracer fuel elements are used, fluctuations are low (see Fig. 34 b). Due to the MEDUL fuel strategy, the core is homogenized to a high extend. Due to this reason, the variations between the regions are very low. A tendency to slightly higher coated particle failure fractions in the lower part of the core can be seen, induced by the higher average burnup level.

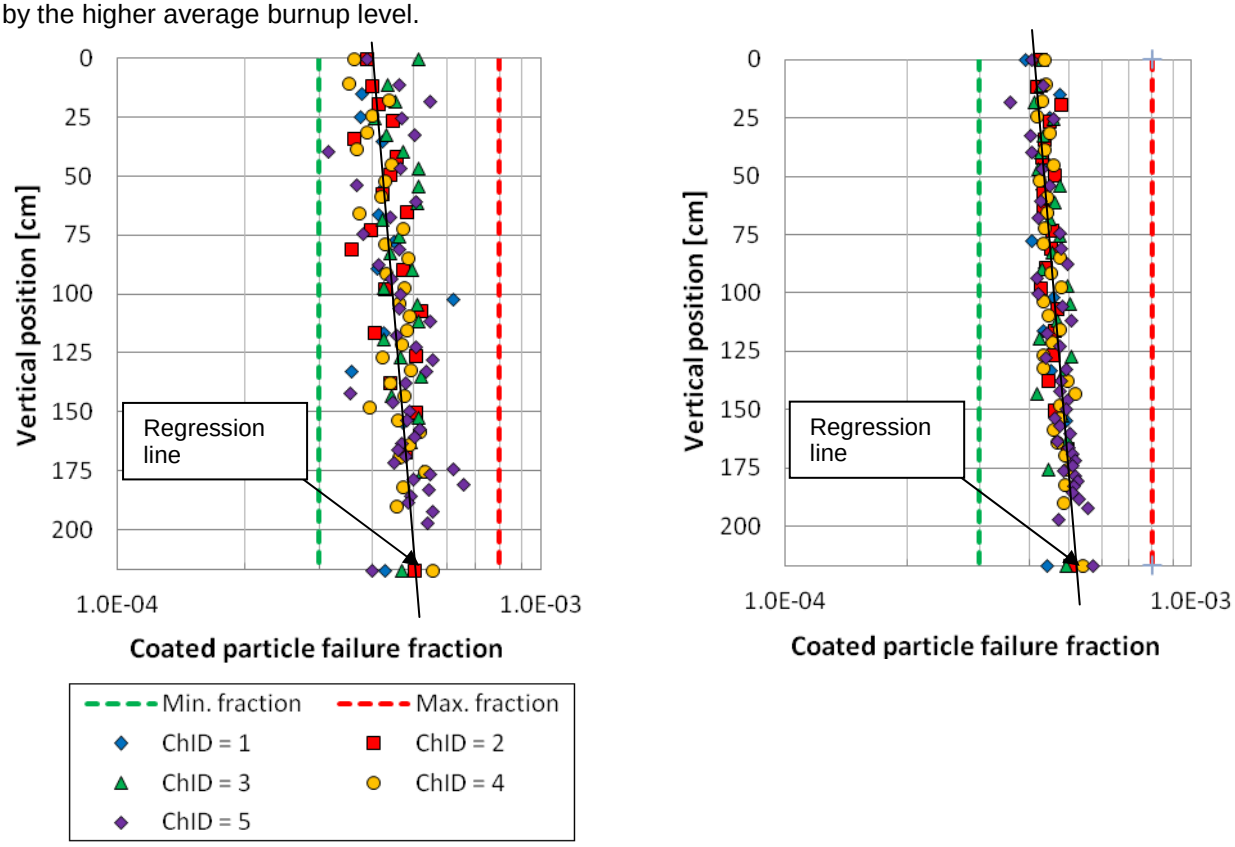

a) 1000 tracer fuel elements within the core b) 4000 tracer fuel elements within the core

Fig. 34: Region-averaged coated particle failure fractions for two different numbers of tracer fuel elements within the core

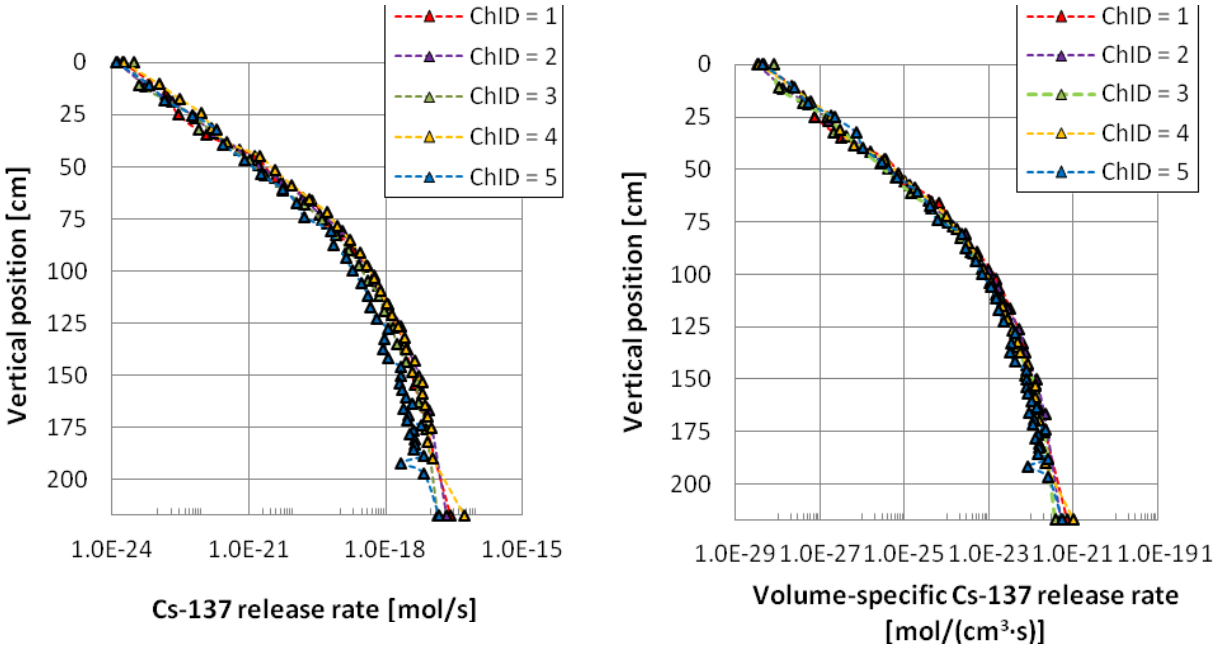

Fig. 35: Absolute and volume-specific cesium 137 release rates within the HTR-10 equilibrium core

Fig. 35 shows the spatial Cs-137 release distribution within the core. It can be seen that the release rates are very comparable for the channels, especially those from the first and second fuel channel. Due to the slightly higher fuel temperatures in the inner part of the core, Cs-137 release rates are highest in the innermost fuel channel.

In addition, volume- specific Cs-137 release rates are shown because each fuel channel has different region volumes (see Table 11).

Table 11: Region volume for each fuel channel

Channel-ID	Volume of one region [cm^3]	Region volume in comparison to region of channel 1 [%]
1	37134	100
2	40479	109
3	37688	101
4	51266	138
5	26951	73

For each of the nuclides being investigated, Cs-137, Sr-90, I-131 and Ag-110m, such a time-depending curve is being calculated. Only the release rate of the equilibrium core is of interest, the time-depending function shown in Fig. 33, before the equilibrium core state has been reached, does not show the release rates during the running-in phase. The release rates from the equilibrium core are displayed in Table 12. Both fission product release rates being calculated by using STACY (FZJ) and those being published in [12] by INET are displayed.

Table 12: Fission product release rates in the HTR-10 equilibrium core

	Cs-137	Sr-90	Ag-110m	I-131
	[Bq/(MW_t·h)]	[Bq/(MW_t·h)]	[Bq/(MW_t·h)]	[Bq/(MW_t·h)]
INET	8.9×10^{3}	2.5×10^{-1}	1.5×10^{2}	4.9×10^{6}
FZJ	5.2×10^{1}	8.7×10^{-2}	2.5×10^{-1}	9.6×10^{5}
INET / FZJ	1.7×10^{2}	2.9×10^{0}	6.0×10^{2}	5.1×10^{0}

No precise data are available regarding the boundary conditions being used for the fission product release calculation being published in [12]. The paper does not mention e.g. the diffusion coefficients applied and the uranium contamination of the different coated particle layers on one hand and the graphite grains and pores (graphite grain boundaries) on the other hand. For this reason, a detailed comparison between the results in [12] and results calculated by using STACY cannot be made. Next, no spatial temperature distribution is given, which does not allow for a reproduction of the calculations performed.

The inventory calculation after both approaches results in comparable values for long-lived fission products. Thus, the fission product release calculation is not affected heavily by this. The fission product release of long-lived nuclides is mainly affected by taking the fuel temperature and nuclide inventory distribution into account. The STACY approach results in lower fission product release rates for those nuclides (see Table 12). Especially the fission product release rates of Cs-137 and Ag-110m are about two magnitudes lower.

In addition to the spatially resolved calculation, there is a second effect which affects the fission product release calculation of short-lived nuclides. Due to the simplified calculation of the nuclide inventory in FRESCO-II, the equilibrium inventory of a short-lived nuclide is achieved after a few days. From this time point, the inventory of a short-lived nuclide is constant. In case of reactor with a MEDUL fuelling strategy, each fuel element is shuffled through the core and is exposed to a time-depending neutron flux. Due to this, the neutron flux increases at the beginning of each core pass and the rate at which a short-lived nuclide is being produced is higher than the rate at which the nuclide is being removed due to decay. At the end of each core pass, the neutron flux decreases and the removal rate is higher than the production rate. Thus, the inventory is periodic and the maximum inventory is located in the middle part of the core.

By assuming an almost constant nuclide inventory for short-lived nuclides, the fission product release rate is not being affected by the inventory itself. In this case, the fission product release rate is merely a function of the fuel temperature and the coated particle failure rate. Due to the MEDUL fuelling strategy, there is no broad distribution of coated particle failure fractions. The average coated particle failure fraction increases only slightly from the upper boundary towards the lower boundary of the pebble bed. Thus, the fission product release rate distribution is mainly affected by the temperature distribution and fission product release rates are highest at the position where the fuel temperatures are highest. In case of a reactor where the coolant flows downwards, the maximum fuel temperature is located in the lower part of the core. Thus, by applying the simplified equation, the position of the maximum fuel temperature does coincide with the position where the nuclide inventory is highest. This results in higher release rates.

STACY performs a fission product release calculation for a large number of tracer pebbles. By doing so, the code takes spatial distributions such as neutron flux distributions, nuclide inventory distribution and fuel temperature distributions into account. Instead, FRESCO-II is mainly used for a limited number of user-defined pebbles. Most of the time, conservative assumptions were used to gain some upper limit for fission product release rates. In [12], the nuclide inventories have been derived from one depletion calculation with ORIGEN-2 for a fuel element which goes merely through the third fuel channel. The paper stresses, that conservative assumptions have been made to calculate fission product release rate without mentioning them in detail.

4.2.2.2 Running-in phase

As an important part of the fission product release calculation, the time-depending nuclide inventories are calculated. The time-depending neutron fluxes are being determined by the STACY based on the VSOP output for each tracer pebbles. These tracer pebbles are shuffled through the core according to the fuel management schemes being defined in the VSOP input file.

The fuel shuffling in the running-in phase calculation differs from the equilibrium core calculation. In case of the equilibrium core, there are no tracer pebbles in the core at the beginning of the calculation, but they are shuffled gradually into the core (like monitor spheres in the melt-wire experiment). In case of the running-in phase, core conditions are changing permanently. For this reason, tracer pebbles have to be tracked during their life history starting from the equilibrium core. At the beginning of the running-in phase calculation, tracer pebbles are loaded to the core. In case of the HTR-10 this means that in the cylindrical part, there is a mixture of tracer elements (representing the fuel) and dummy tracer elements (representing the dummy elements). In the lower part of core, there are solely dummy tracer elements. Fig. 36 shows the initial HTR-10 core containing a large amount of tracer elements (“o”) and dummy tracer elements (“+”).In this picture, the three dimensional positions of the pebbles are condensed to a two dimensional picture. By doing so, the density of tracer pebbles is higher at larger radii.

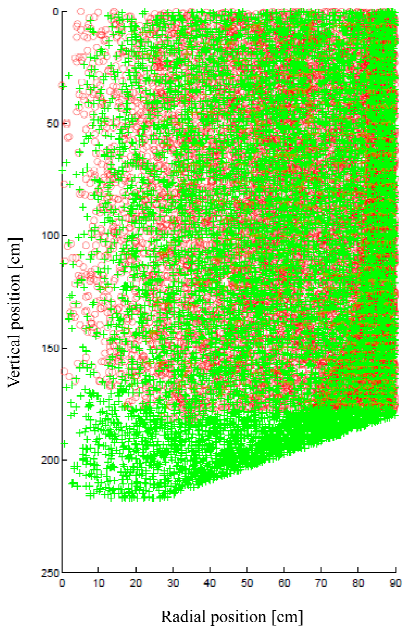

Fig. 36: Snapshot of the initial HTR-10 core in STACY
(green “+”-symbol : dummy tracer elements; red circle : fuel tracer element)

Neutron flux distributions

In case of the equilibrium core, a constant neutron flux distribution is used to generate the time-depending broad group fluxes for each individual tracer pebble. Due to the fact that the composition of the core regions varies over time and the reactor is being operated at different power levels, the neutron flux distributions vary over time during the running-in phase. For this reason, the broad group neutron flux distributions are read for each fuel shuffling time step from the VSOP output file. Fig. 37 shows the spatial thermal neutron flux distributions of both the initial and equilibrium core at nominal power (10 MW). It is obvious that the flux distribution is affected by the content of the regions. Within the initial core, there is a clear spot where the thermal flux is highest. The equilibrium core is homogenized which is reflected in the neutron flux distribution.

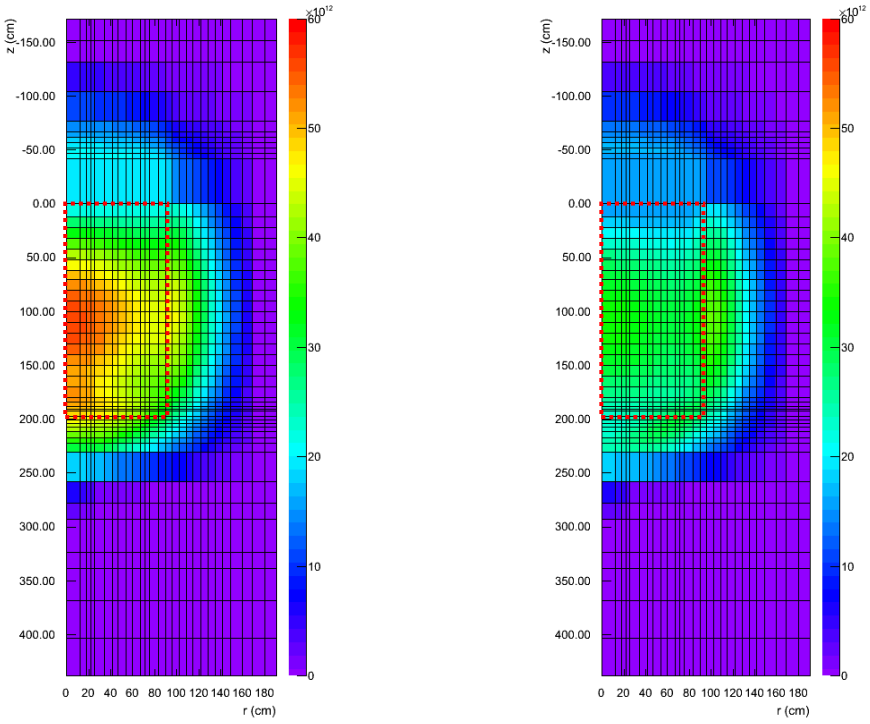

Initial core
at 10 MW_{th}

Equilibrium core
at 10 MW_{th}

Thermal flux
($2.5x10^{-3}$ eV < E ≤ 1.9 eV)

Fig. 37: Spatial thermal neutron flux distributions within the HTR-10 initial and equilibrium core

Fuel temperatures

Comparable to the neutron fluxes, for each time, a temperature distribution is used. The temperature distributions within the initial core and equilibrium core are shown in figure Fig. 38. It can be seen that in most areas of the core, fuel temperatures are higher in the initial core compared to those in the equilibrium core.

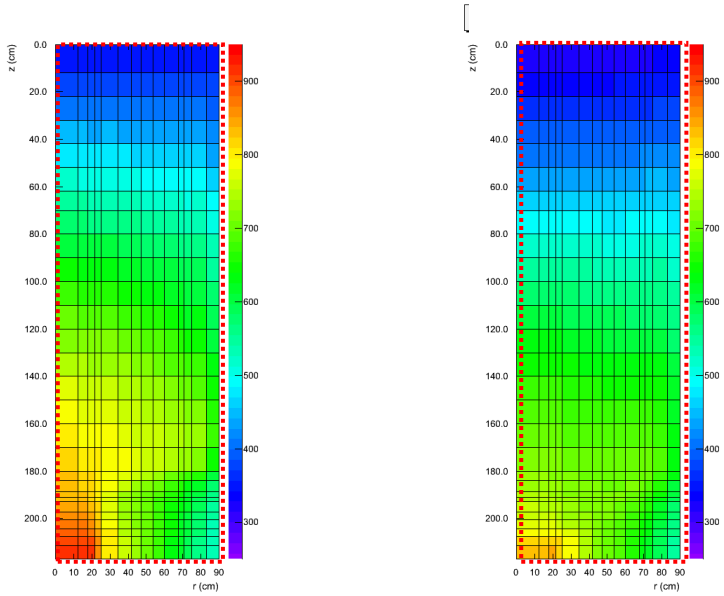

Initial core at 10 MW_{th}

Equilibrium core at 10 MW_{th}

Fig. 38: Spatial central fuel temperature distributions within the HTR-10 initial and equilibrium core

Fuel shuffling

An important aspect of the fission product release calculation is the correct description of the fuel management, because the life history of each individual tracer pebble depends mainly on the time-depending position through the active core. After the fuel shuffling code module in STACY has been extended to enable fuel shuffling during the running-in phase, a verification process has been conducted to verify implementation. As an example, the content of the core is being displayed for two time steps in Fig. 39. In comparison to the calculation itself, which is based on 4000 fuel elements, only 1000 fuel elements are being displayed here. Fig. 39 shows the core content after the time step 3, at which fuel elements are reintroduced to the core for the first time (blue circle). Due to the limited number of spheres and the randomness added by the Monte-Carlo approach, no fuel elements are added to the fourth and fifth fuel channel. As another example, the core content after 15 fuel shuffling steps is displayed. During the first two fuel shuffling steps a mixture of fresh fuel elements (red circle) and dummy spheres (green “+”-symbol) is added to the core. After these two fuel shuffling steps, no dummy spheres are added to the core. The first channel contains 14 regions. Due to this, after 15 fuel shuffling steps, the dummy spheres have reached the lowest region of fuel channel one.

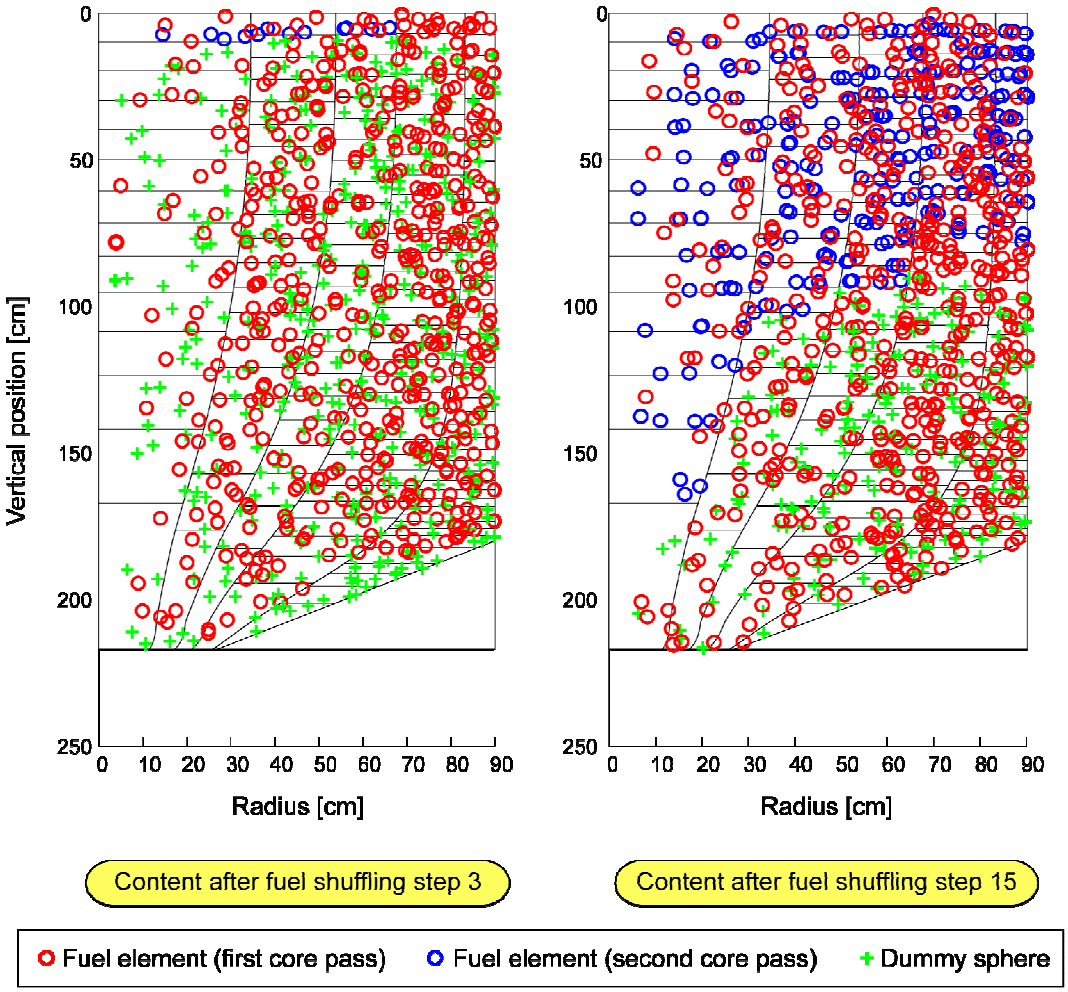

Fig. 39: Tracer pebble content at the end of fuel shuffling step 3 and 5

The operating history of the HTR-10 is displayed in Fig. 40. The figure shows whether the reactor was in an operating- or shutdown-phase and not the power at which the reactor was operated, because the magnitude of the fluxes depends on both the position of the fuel element and the power level at which the HTR-10 was operated. This means that even if the reactor is being operating at a higher power level, the fluxes can be lower in comparison to a time point at which the reactor was operating at a lower power level due to the fuel elements' position.

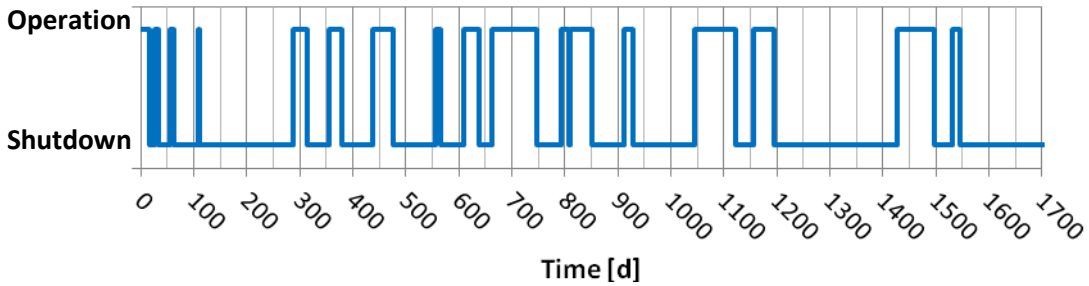

Fig. 40: Operating history of HTR-10

First, different results of one randomly selected fuel element will be presented. Fig. 41 shows the broad group fluxes of this fuel element during the running-in phase. This fuel element is part of the initial core and was about to finish its final core pass before the reactor operation was paused. The shutdown phases can be seen clearly. In comparison to the diagram showing the operating history (see Fig. 40), Fig. 41 contains more individual levels, due to the fact that the fluxes are adapted as soon as the lower boundary of a region is crossed.

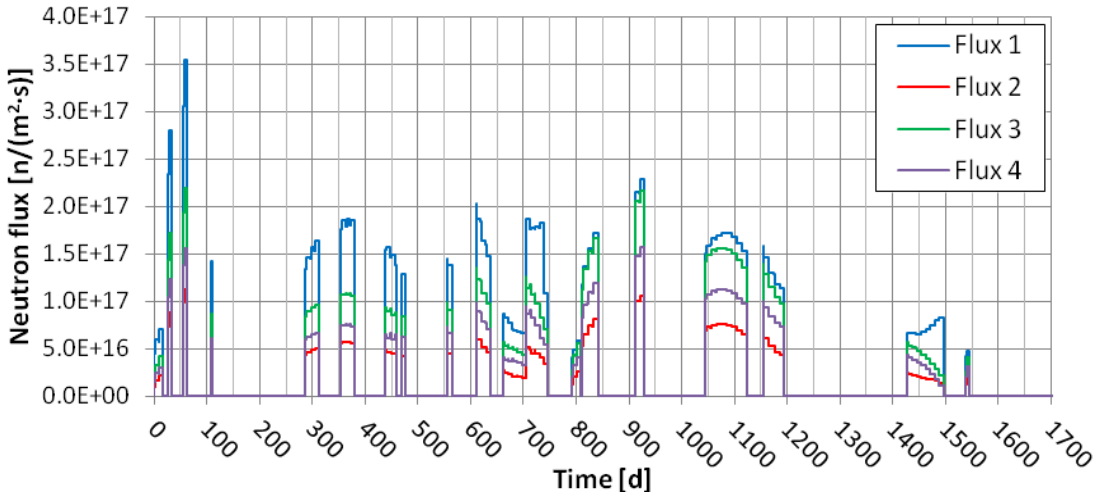

Fig. 41: Broad group fluxes of one HTR-10 fuel element during the running-in phase (see figure Fig. 29 for the energy boundaries of the broad group neutron fluxes)

The burnup calculations are performed by using the TNT code. The inventories of Sr-90, Cs-137 and I-131 are displayed in Fig. 42. The long-lived nuclides Sr-90 and Cs-137 do only decay to a negligible amount during the shutdown phases. The short-lived nuclide I-131 decays in some longer shutdown phases completely. Due to the time step widths chosen, the exponential shape of the time depending inventories cannot be recognized.

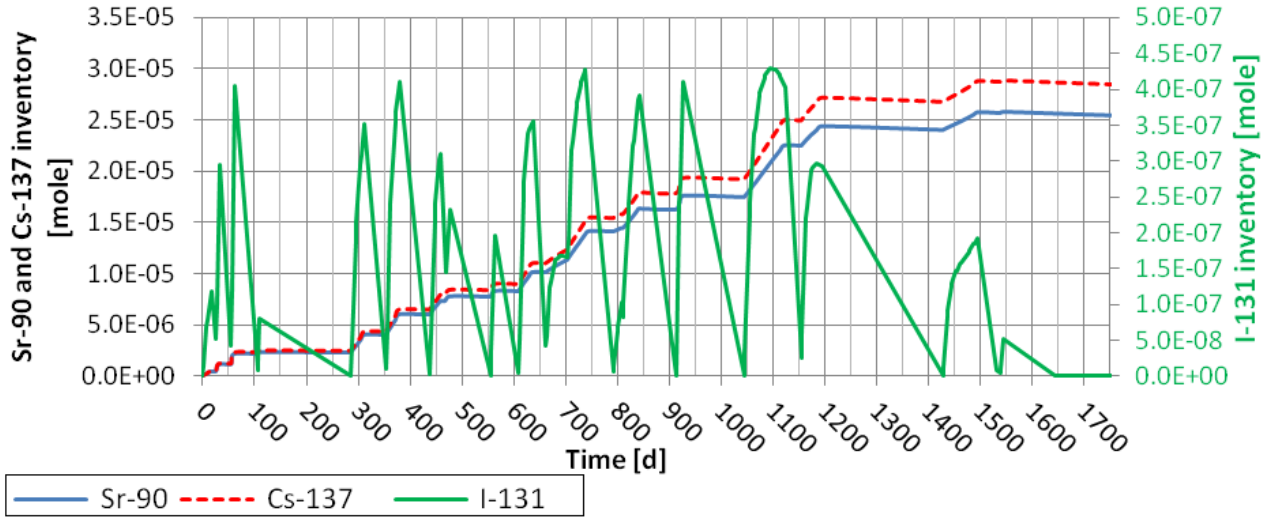

Fig. 42: Strontium 90, cesium 137 and iodine 131 inventory of one HTR-10 fuel element during the running-in phase

Fig. 43 shows the position of a random tracer fuel element during the running-in phase and demonstrates the quasi-continuous movement of the tracer. This fuel element is part of the initial core and is located in the uppermost region of the most inner fuel channel. During its second core pass, the fuel element flows along an interpolated flow curve which is positioned in the second fuel channel and during the third core pass the fuel element flows through the outermost fuel channel. There it resides since the final shutdown phase.

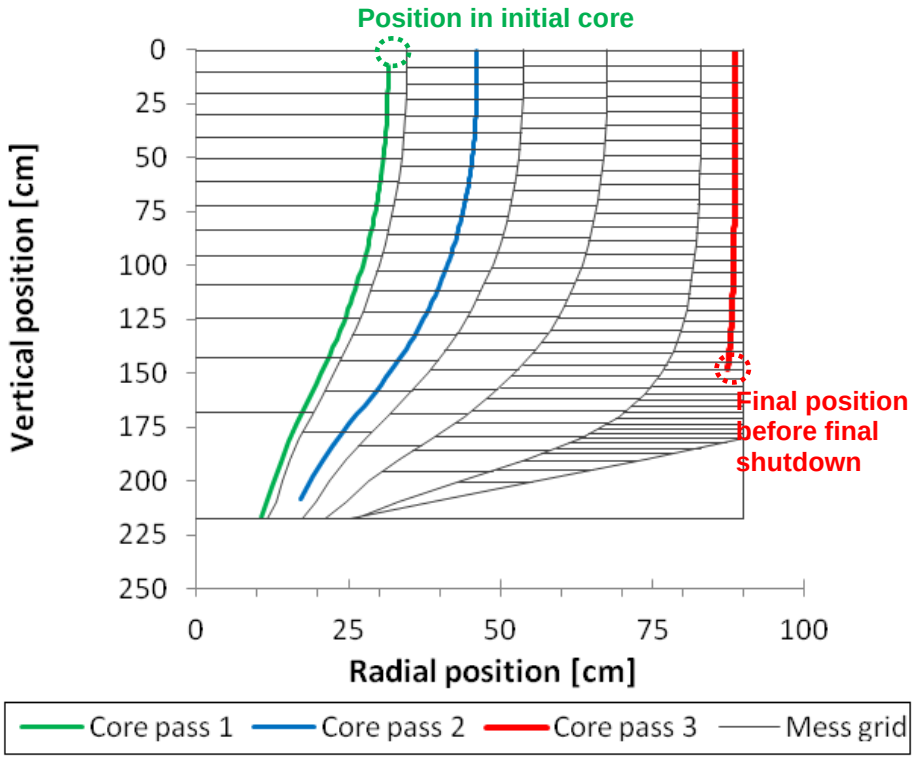

Fig. 43: Position of a random tracer fuel element during running-in phase of HTR-10

Fig. 44 shows both the vertical and radial position of a random tracer element as a function of time.

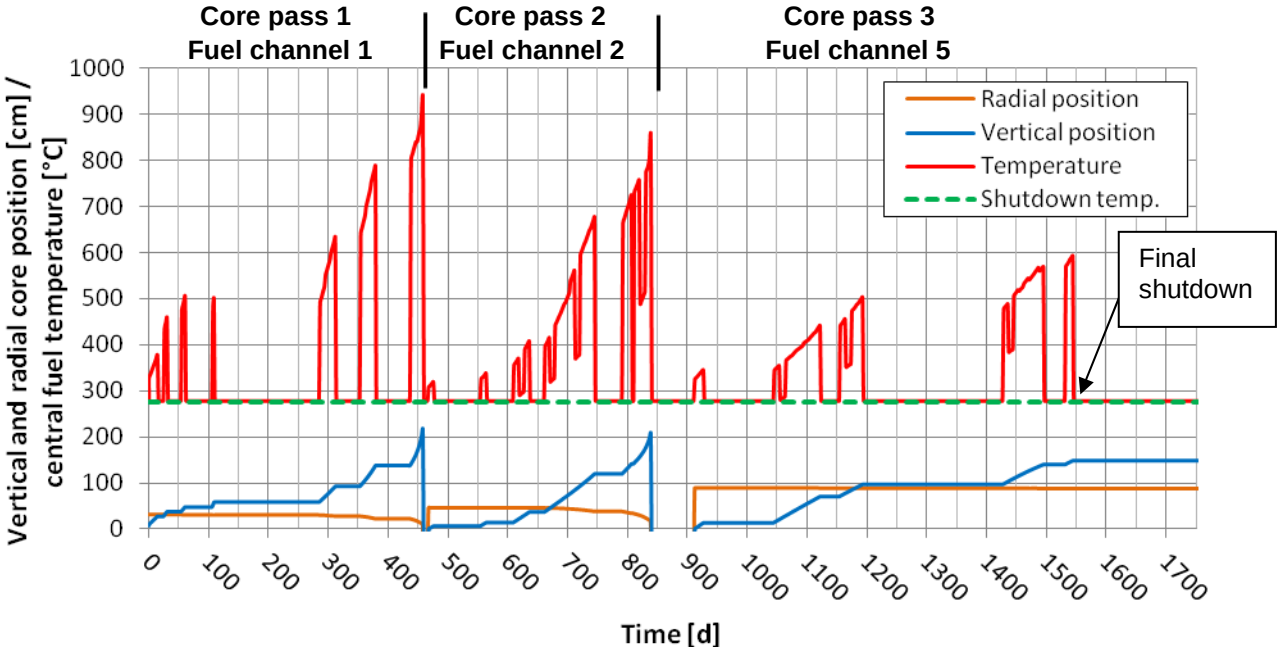

Fig. 44: Position and central fuel temperature of a random tracer fuel element during running-in phase of HTR-10

It can be seen that the fuel elements do not move during shutdown phases. The radial position decreases gradually at the end of each core pass. In case of the equilibrium core the residence time within the second fuel channel is shorter in comparison to the residence time within the first fuel channel because the core is being shuffled continuously. In case of the running-in phase, the residence time is shorter in the second fuel channel than in the first fuel channel due to longer shutdown phases at the beginning of reactor operation. After being discharged at the end of the second core pass, the tracer element resides for approximately 50 days in the fuel handling system (out-of-core box), because after discharge, the core is shutdown.

In addition, the central fuel temperatures are shown in Fig. 44. During each core pass, the central fuel temperature increases gradually. The power level at which the reactor is being operated has only a minor effect on the fuel temperature. During shutdown phases, a constant fuel temperature is being used. This is necessary because THERMIX calculations do not converge during a shutdown phase. This constant temperature does not take into account that the fuel temperature during shutdown phases is both depending on the position of the fuel element and the time-depending decay power. Nevertheless, during shutdown phases, fuel temperatures decrease rapidly and are rather low. For this temperature range, the diffusion coefficients of the nuclides of interest do not depend heavily on the "exact" fuel temperature. Thus, a constant temperature is a good approximation for these operating phases.

Fig. 45 shows the burnup and neutron influence of the same random fuel element. This fuel element achieves a burnup of approximately 2.3 % FIMA and collects a neutron fluence of 0.3×10^{25} n/m^2. VSOP simulation of the HTR-10 equilibrium shows up that the neutron fluence at the end of life is approximately equal to 1.13×10^{25} n/m^2. The burnup level affects the coated particle failure fraction. The neutron fluence has only little influence on calculated results. Only the diffusion coefficient of cesium is slightly influenced by the neutron fluence.

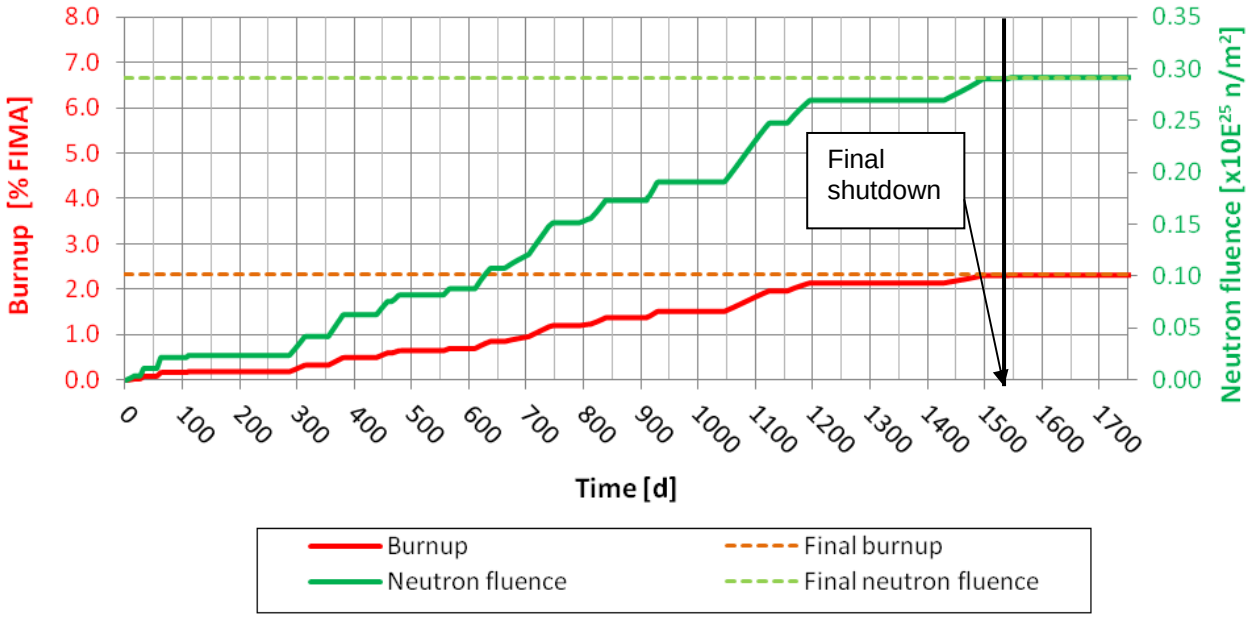

Fig. 45: Burnup and neutron fluence of a random tracer fuel element during running-in phase of HTR-10

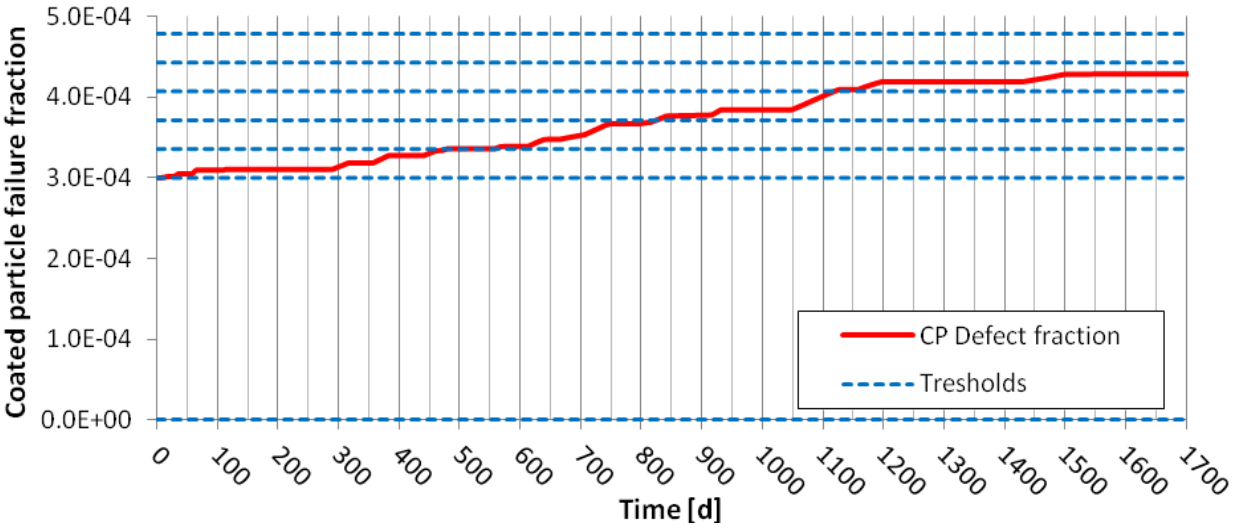

Fig. 46: Coated particle failure fraction of random tracer pebble during running-in phase of HTR-10

The time-depending coated particle failure fraction is shown in Fig. 46. In addition, the threshold being used within the calculation can be seen.

Combining these results from all tracer-elements results in the fission product release rates of the complete core during the running-in phase. A fission product release calculation is only conducted for the fuel elements. The deposition on and diffusion into dummy elements is neglected. The dummy elements are shuffled by the fuel management to have a correct representation of the content of each region, to enable a correct scaling of the fission product release rates from the individual tracer pebbles to overall core release rates. The time-depending Cs-137, Sr-90, Ag-110m and I-131 release rates are shown in Fig. 47, Fig. 48, Fig. 49 and Fig. 50, respectively. All power specific release rates have been determined with respect to the nominal power of 10 MW_{th}. In addition to the time depending release rates during the running-in phase the release rates of the equilibrium core has been added. All the figures show, that as soon that the reactor is shut down, the release rate decreases by about several orders of magnitude. This holds for both the short- and long-lived nuclides. In addition, even during the shutdown phase, the release rates of the short-lived nuclides decrease due to the removal of the fission products of interest by decay. Due to the fact that the inventory of long-lived nuclides is practically constant during these shutdown phases and temperatures changed are neglected, fission product release rates of long-lived nuclides are nearly constant.

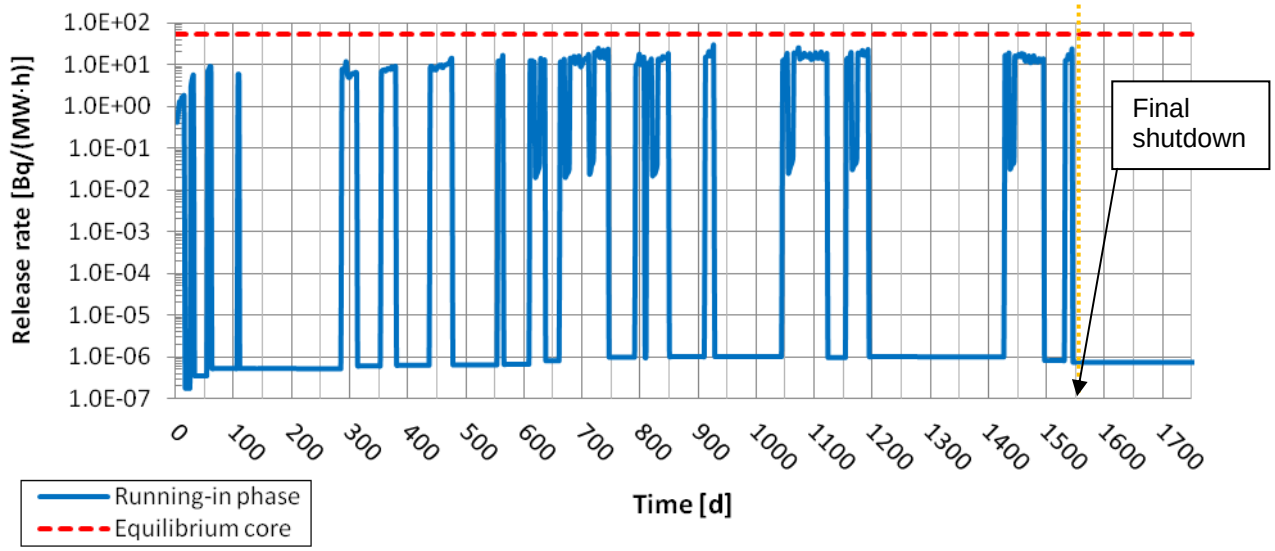

Fig. 47: Cesium 137 release rate during the running-in phase

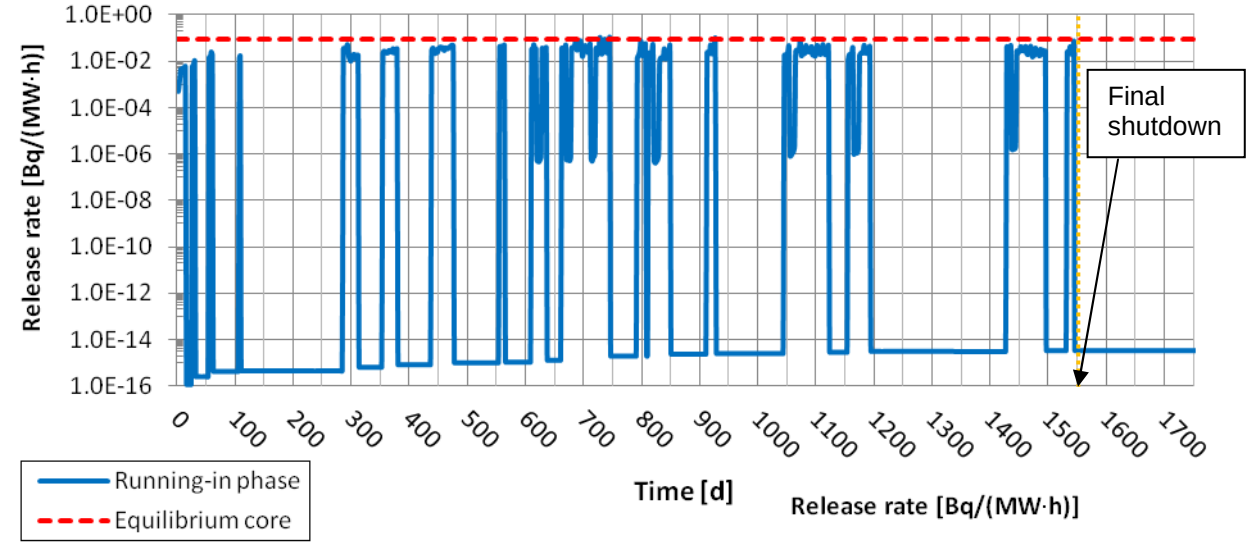

Fig. 48: Strontium 90 release rate during the running-in phase

The power level at which the HTR-10 is being operated varies within one magnitude. Due to the fact that there are no clear temperature peaks during the running-in phase, maximum release rates do not vary over many magnitudes during operating phases.

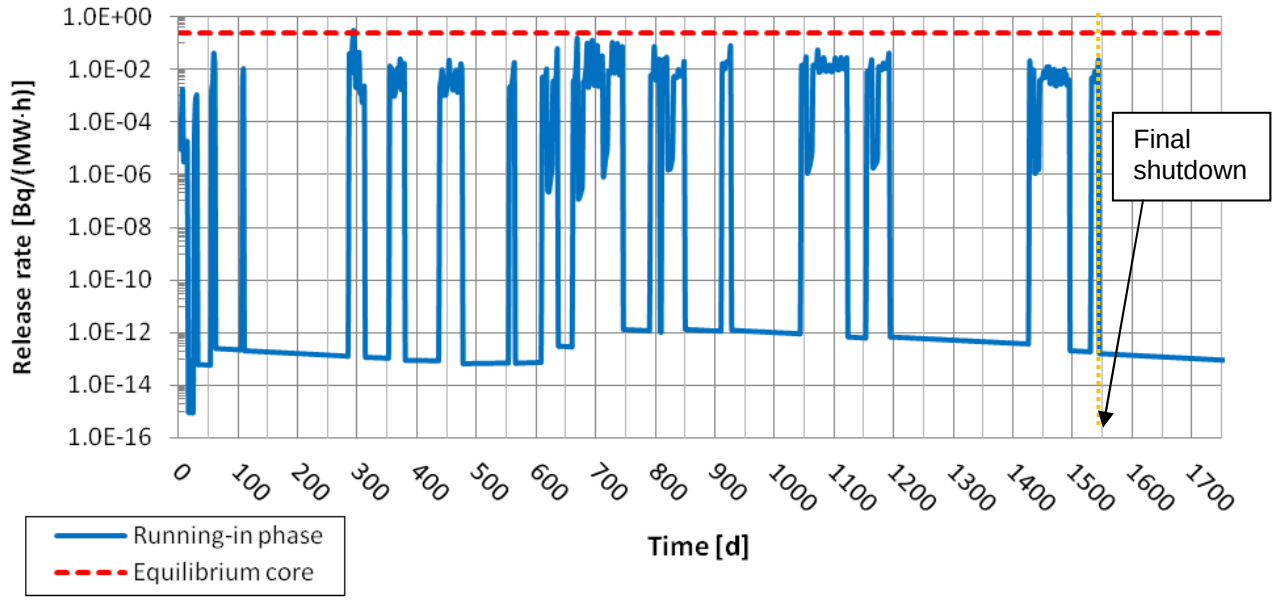

Fig. 49: Silver 110m release rate during the running-in phase

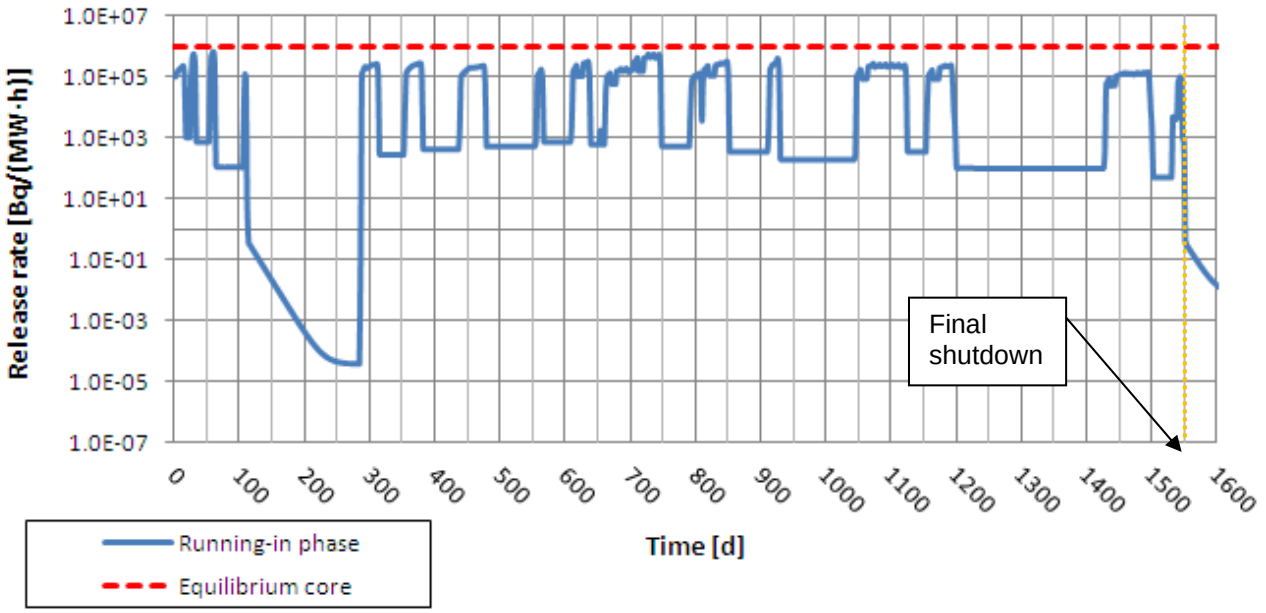

Fig. 50: Iodine 131 release rate during the running-in phase

Finally, an exemplary comparison of spatially resolved Cs-137 release rates is shown in Fig. 51. For each core region, an average release rate of all tracer elements within is being determined. As mentioned earlier, for a tracer fuel element the fission product release rate is calculated, for dummy elements, the release / deposition rate is neglected and set to zero. Attention should be being paid to the fact that the absolute release rates are being shown and not the volume-specific ones.

While the plant is being operated, the fuel temperatures are highest within the lower part of the core. For this reason, a clear tendency towards higher release rates in the lower part of the core can be seen. A few hours after the core has stopped operation, fuel temperatures are more even distributed and a shift from the

location of the maximum fuel temperature from the lower part of the core (during operation) towards the centre (where decay power is highest) can be detected. Accordingly, the maximum of the Cs-37 release rate moves towards the centre and due to the lower absolute temperatures, release rates are lower within each region. During operation, the release rate is higher in the inner fuel channels, which is caused by the higher fuel temperatures. During the shutdown phase, the fuel temperatures are more even. Due to this, the release rate is dominated by the inventories of the spheres, which are higher in the outer fuel channel due to the longer residence times (see Fig. 51).

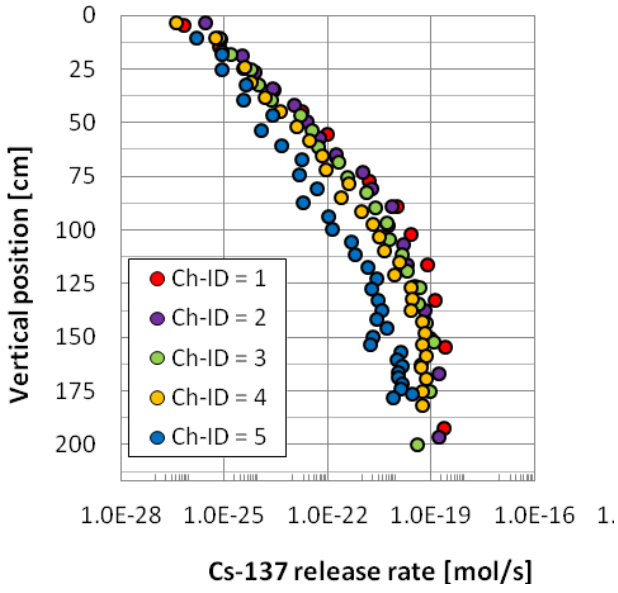

a) 4.5 hours (HTR-10 in operation)

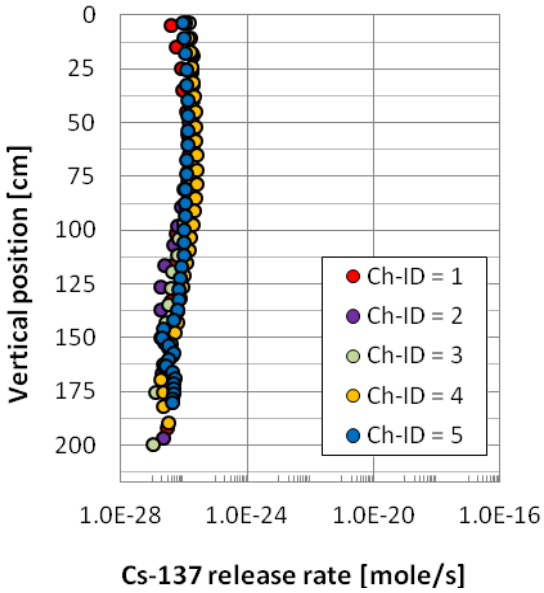

b) 16.0 hours (HTR-10 first shutdown)

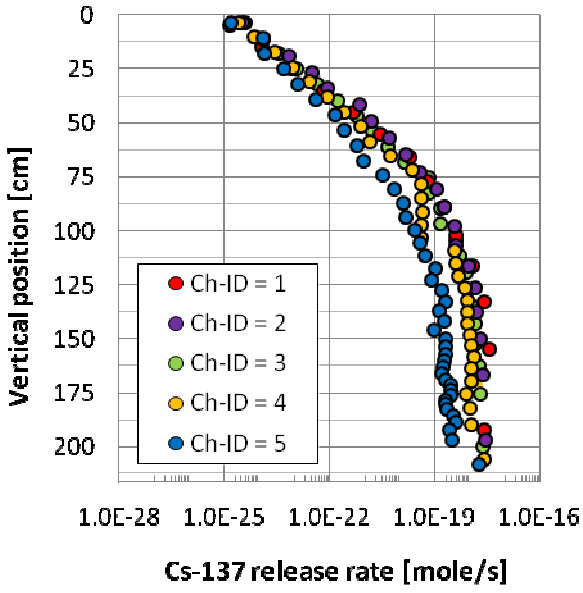

c) 562.5 hours (HTR-10 in operation)

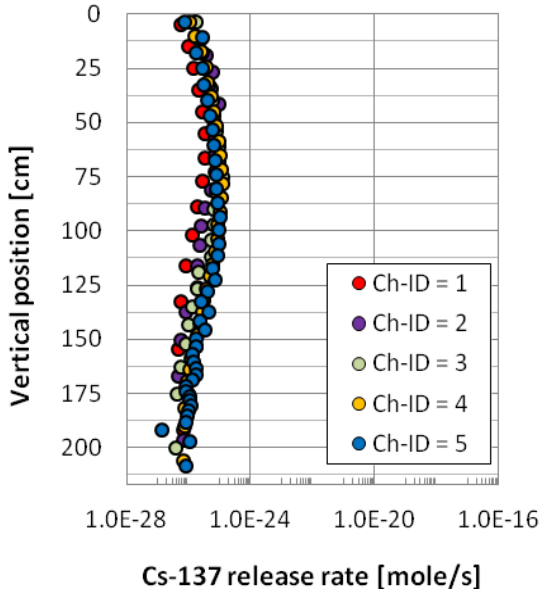

d) 565.0 hours (HTR-10 shutdown)

Fig. 51: Spatially resolved cesium 37 release rates before and shortly after one reactor shutdown during the operating history of the HTR-10

After 562.5 hours, the total Cs-137 inventory within the core in still increasing, because no fuel elements have been discharged yet. Due to this, even if the power level at which the reactor is being operated is

comparable, the fission product release rate at higher after 562.5 are higher in comparison to those after a few hours of operation (see Fig. 51a).

5 Conclusions

Within this work, the fission product release of the HTR-10 over its operation time was simulated. The fuel temperature distribution and the fission product inventory distribution which serve as input to the STACY calculation are generated by a coupled neutronics and fluid dynamics calculation with VSOP99/09. Within this calculation, the power histogram published by INET and additional assumptions based on the HTR-Module-200 were taken as further input. Especially the applied shuffling scheme (modelled on the basis of the considerations in [10]) is purely theoretical and not supported by experimental data. However, it should be noted that with the available data and the assumptions made, a consistent model could be established.

STACY is a code, which calculates the fission product release of an HTR core by taking into account a large number of so called tracer pebbles. The STACY model developed in [15] has been extended for this study in such a way, that all core states can be treated. This extended STACY version has been used to calculate the fission product release rates of Cs-137, Sr-90, I-131 and Ag-110m within the HTR-10 for both the running-in-phase and the equilibrium core.

Fission product release rates have been published by INET only for the HTR-10 equilibrium core. No data regarding the fission product release during the actual operation history is available. For this reason, only a comparison can be conducted for the equilibrium core. Due to the fact that it is not clear which diffusion coefficients have been applied within the INET calculation, it has been assumed that diffusion coefficients proposed by TECDOC 978 have been applied. In comparison to the INET calculations, the release rates of all investigated nuclides are lower in the equilibrium core. The release rate of Sr-90 is about a factor of 3, the rate of Cs-137 about a factor of 170, the rate of I-131 about a factor of 5 and the release rate of Ag-110m about two magnitudes lower. These discrepancies can be explained by the fact that in former studies only a few fuel elements have been analyzed. The fuel elements are exposed to maximum fuel temperatures. Results from these individual calculations have been extrapolated to derive specific release rates for the whole active core. In comparison to the INET calculations, in the new STACY approach, the spatial distributions of e.g. fuel temperatures and nuclide inventories are taken into account instead of maximum values only. This results in the lower fission product release rates within the simulation. During the actual operation phase, the fission product release rates are comparable to those of the equilibrium core as long as the reactor is operated. After shutdown, the release rates decrease rapidly.

Nevertheless, measurements comparable to the VAMPYR experiments conducted within the AVR are required to validate the overall fission product release results of the HTR-10.

Literature

[1] IAEA. (2003). *Evaluation of high temperature gas cooled reactor performance. Benchmark analysis related to initial testing of the HTTR and HTR-10.* Wien: IAEA-TECTDOC-1382.

[2] Druska C., S. S. (2012). *Simulation of the Equilibrium Core and Steady State of the HTR-10.* Jülich: ARCHER deliverable D24.11.

[3] Rütten H.J., H. K. (2010). *V.S.O.P. (99/09) Computer Code System for Reactor Physics and Fuel Cycle Simulation, Version 2009.* Jülich: Forschungszentrum Jülich, 4326.

[4] LI, F. (2011). The HTR-10, operation performance and data collected. *IAEA Consultancy Meeting on the Performance of Past and Present HTGR Test Reactors and Critical Facilities, Vienna, 5-7 December 2011*.

[5] NEA. (2006/2007). *Evaluation of the initial critical configuration of the HTR-10 pebble-bed reactor.* NEA/NSC/DOC(2006)1.

[6] Jing X., Y. Y. (2004). Physical Designs and Calculations for the First Full Power Operation of the 10MW High Temperature Gas-Cooled Reactor-Test Module (HTR10). *2nd International Topical Meeting on HIGH TEMPERATURE REACTOR TECHNOLOGY.* Beijing.

[7] Siemens-Interatom. (1989). *Part load diagram of HTR-Module.* Bergisch Gladbach: HTR-Modul-Konzeptunterlagen.

[8] Siemens-Interatom. (1988). Safety Analysis Report

[9] Gao Z., S. L. (2002). Thermal hydraulic calculation of the HTR-10 for the initial and equilibrium core. *Nuclear Engineering and Design 218*, S. 51-64.

[10] Yang, Y. (2002). Fuel management of the HTR-10 including the equilibrium state and the running-in phase. *Nuclear Engineering and Design 218*, S. 33-41.

[11] Leppänen, J. (2013). *Serpent - a Continous-energy Monte Carlo Reactor Physics Burnup Calulation Code - User Manual.* Finland: VTT Technical Research Center in Finland.

[12] Liu Y., J. C. (2002). Fission Product Release and its environment impact for normal reactor operations and relevant accident. *Nuclear Engineering and Design 218*.

[13] IAEA. (1997). *Fuel Performance And Fission Product Behavior in Gas Cooled Reactors.* Wien: IAEA-TECDOC-978.

[14] Herber S.C., F. N.-J. (2012). First Steps towards a Validation of the New Burnup and Depletion Code TNT. *Annual Meeting on Nuclear Technology.* Stuttgart.

[15] Krohn H., F. R. (1983). *FRESCO-II - Ein Rechenprogramm zur Berechnung der Spaltproduktfreisetzung aus kugelförmigen HTR-Brennelementen in Bestrahlungs- und Ausheizexperimenten.* Jülich: Forschungszentrum Jülich, Interner Bericht.

[15] Xhonneux A., *Räumlich hoch aufgelöste Modellierung der Spaltproduktfreisetzung aus einem HTR Core mit kugelförmigen oder prismatischen Brennelementen*, PhD RWTH-Aachen, 2013

[16] IAEA: *Fuel Performance and Fission Product Behaviour in Gas Cooled Reactors*, IAEA-TECDOC-978, Wien, 1997